tremoFlo N-100®: A device to measure lung function in infants

by

Farah Al-Huda
Division of Experimental Medicine
McGill University, Montreal, Quebec, Canada
December 2022

A thesis submitted to McGill University in partial fulfillment of the requirements of the degree of Master of Science

Table of Contents

Abstract

Background: Currently available commercial oscillometers, like the tremoFlo® C-100, can only be used in adults and children aged at least two years old. However, no devices exist for infants. The tremoFlo® C-100 was modified to enable its use in infants, leading to the development of the tremoFlo® N-100 Airwave Oscillometry System™.

Aims: 1. To validate the new tremoFlo® N-100 by comparing its spectral measurements of respiratory impedance (Z_{rs}), specifically resistance (R_{rs}) and reactance (X_{rs}), with those of the current gold standard OSC device for infants, the Wave-tube Oscillometer. 2. To identify physiologically meaningful intra-breath patterns of respiratory mechanics by analyzing Z_{rs} at 16 Hz.

Methods: A total of 27 healthy, term (> 37 weeks) infants, with no neonatal or respiratory issues were enrolled. Internal validation of the tremoFlo® N-100 involved 14 infants (9 females, 5 males), while external validation with the wave-tube involved 13 infants (7 females, 6 males). R_{rs} and X_{rs} (at 7, 13, 19, 29 and 37 Hz), frequency dependence of R_{rs} (R_{7-19} and R_{7-29}), resonant frequency (f_{res}) and reactance area below f_{res} (AX) were averaged from at least three 10-30s, artefact-free segments from both devices. They were compared using intraclass correlation coefficient (ICC) and Bland-Altman Limits of Agreement. Intra-breath analysis was conducted on data at 16 Hz.

Results: The first part of the study showed that the more regular breathing pattern during sleep improved coherence (COH), while adding a bias flow improved coefficient of variation (CV) by flushing equipment dead space. There was no correlation between impedance and height, weight or sex. In the second part of the study, the measurement duration was extended, which proved more practical and accurate. Reasons for data exclusion included inadequate sleep state (3), testing with one device (2) and testing in stroller (2). Spectral impedance data were all within the reproducibility threshold. Sufficient spectral data measured by each device for 4 infants were analyzed with ICC and Bland-Altman Limits of Agreement. Sufficient intra-breath data from both devices were collected and compared from 1 infant. Due to the small sample size, results should be cautiously interpreted. Reliability based on ICC showed X37 had excellent reliability, while X19, X29, R7-19 and AX had modest reliability. Bland-Altman plots revealed an outlier but indicated close agreement.

Discussion: Based on reproducibility measures of COH and CV calculated by the internal tremoFlo® software, testing sleeping infants using a bias flow resulted in optimal data collection. The ideal testing position was one in which the infant was horizontal and avoided neck flexion.

The small sample size of inter-device comparison highlights the importance of a favourable environment conducive to testing infants, free of time constraints, as well as a dedicated, consistent team of more than one person.

When compared with the wave-tube, both spectral and intra-breath recordings of the N-100 systematically underestimated resistance, but adequately measured reactance. Potential solutions include refitting the gain and zero offset errors of the N-100's sensors using a stable flow bench system, correcting for mask impedance and modifying the resistance component of the three-point model. In contrast to ICC, Bland-Altman showed AX as having the largest measurement error.

Resistance at all frequencies using the N-100 was higher than the modified C-100. Using higher calibration test loads and oscillations with higher amplitudes may have enhanced accuracy. Reactance at all frequencies using the N-100 was less negative than the modified C-100, which may be due to the difference in study population age.

Conclusion: With some modification and further validation, the tremoFlo® N-100 is poised to serve as the standard device for infant oscillometry research studies and eventually routine clinical use.

Résumé

Contexte : Contexte : Les oscillomètres commerciaux comme le tremoFlo® C-100 sont indiqués pour les adultes et les enfants de deux ans ou plus - aucun appareil n'existe pour les nourrissons. Le tremoFlo® C-100 a été modifié pour permettre son utilisation chez ces derniers, ce qui a mené au développement du tremoFlo® N-100 Airwave Oscillometry System™.

Objectifs : 1. Valider le système tremoFlo® N-100 en comparant ses mesures spectrales d'impédance respiratoire (Z_{rs}) (de résistance (R_{rs}) et de réactance (X_{rs})) avec celles du dispositif OSC de référence actuelle pour les nourrissons, l'oscillomètre Wave-tube. 2. Identifier les modèles intra-respiration physiologiquement significatifs de la mécanique respiratoire en analysant Z_{rs} à 16 Hz.

Méthodes : Un total de 27 nourrissons à terme en bonne santé, sans détresse néonatale ni problèmes respiratoires ont été inclus. La validation interne du tremoFlo® N-100 a impliqué 14 nourrissons (9 F, 5 H), tandis que la validation externe avec le tube à ondes a impliqué 13 nourrissons (7 F, 6 H). R_{rs} et X_{rs} (à 7, 13, 19, 29 et 37 Hz), la dépendance en fréquence de R_{rs} (R7-19 et R7-29), la fréquence de résonance (f_{res}) et la zone de réactance sous fres (AX) ont été moyennées à partir de au moins trois segments de 10 à 30 s sans artéfact des deux appareils. Ils ont été comparés à l'aide du coefficient de corrélation intraclasse (ICC) et des limites d'accord de Bland-Altman. L'analyse intrarespiration a été réalisée sur des données à 16 Hz.

Résultats : Un schéma respiratoire plus régulier pendant le sommeil a amélioré la cohérence, tandis que l'ajout d'un flux de biais a amélioré le coefficient de variation. Il n'y avait pas de corrélation entre l'impédance et la taille, le poids ou le sexe. De plus, la durée de mesure a été prolongée, ce qui s'est avéré plus pratique et plus précis. Les raisons de l'exclusion des données comprenaient un état de sommeil inadéquat (3), des tests avec un seul appareil (2) et des tests dans une poussette (2). Des données spectrales suffisantes mesurées par chaque appareil pour 4 nourrissons ont été analysées avec les limites d'accord ICC et Bland-Altman. Des données suffisantes des deux appareils ont été recueillies et comparées à partir d'un nourrisson. En raison de la petite taille de l'échantillon, les résultats doivent être interprétés avec prudence. Le ICC a montré que X37 avait une excellente fiabilité, tandis que X19, X29, R7-19 et AX avaient une fiabilité modeste. Les tracés de Bland-Altman ont révélé une valeur aberrante mais ont indiqué un accord étroit.

Discussion : Le test des nourrissons à l'aide d'un flux biaisé a abouti à une collecte de données optimale. La position idéale était celle dans laquelle le nourrisson était horizontal et évitait la flexion du cou.

La petite taille de l'échantillon de comparaison met en évidence l'importance d'un environnement favorable pour le dépistage des nourrissons, sans contraintes de temps, ainsi qu'une équipe dédiée et cohérente.

Par rapport au tube à ondes, les enregistrements du N-100 ont systématiquement sous-estimé la résistance, mais ont mesuré adéquatement la réactance. Les solutions potentielles incluent le réajustement des erreurs de gain et de décalage zéro des capteurs du N-100 à l'aide d'un système de banc d'écoulement stable, la correction de l'impédance du masque et la modification de la composante de résistance du modèle à trois points. Contrairement à ICC, Bland-Altman a montré que AX avait la plus grande erreur de mesure.
La résistance du N-100 était plus élevée que le C-100 modifié. La réactance en utilisant le N-100 était moins négative que le C-100 modifié, ce qui peut être dû à la différence d'âge de la population étudiée.
Conclusion : Avec quelques modifications et une validation supplémentaire, le tremoFlo® N-100 est sur le point de servir d'appareil standard pour les études de recherche sur l'oscillométrie infantile et éventuellement pour une utilisation clinique routine.

Acknowledgements

First and foremost, I would like to express my sincerest gratitude for my supervisor, Dr. Larry Lands, and his guidance and support over the last two years.

I would also like to thank Dr. Zoltan Hantos for coming all the way from Hungary and leaving Nicolas (the wave-tube) in our care, as he continued to provide his time and expertise remotely, Dr. Ronald Dandurand for the foundational literature, Dr. Mara Ludwig, my academic advisor, and Dr. Adam Shapiro from my thesis committee.

I thank Natalia Restrepo and Dr. Lennart Lundblad from THORASYS Inc., as well as members of the tremoFlo® N-100 user group for their assistance. Thanks to MEDTEQ (Quebec Consortium for Research and Innovation in Medical Technologies) and THORASYS Inc. for funding this project.

I truly appreciate the support provided by Tracy, Paul, Jen, Elise and Toni at the CIM, as well as Dr. Bashayer Al-Nuaimi and Farah Glessa for help with recruitment, enrolment and testing.

Special thanks to all the study participants and maternity unit nurses at the Royal Victoria Hospital for their cooperation in developing this work.

Last, but not the least, I am so grateful for Olivia Herron, Erika Badeau and my mom for all the emotional support throughout my graduate school journey.

In Grade 10 Careers class, we had to pick a career for the final research project. Coming from a family of physicians, I was always nudged towards medicine, but my default option was already snatched up by my classmate and I ended up with dentistry. To my surprise, the more I looked into it, the more it solidified my resolve to go to dental school. This serendipitous twist of fate led me on years of hurdles, sacrifices and failures, but without them, I wouldn't have the resilience, work ethic and determination I do today. In the middle of my MSc, I finally got in! So, to 15-year-old Farah, I'd like to say: we did it!

Contribution of Authors

Study conception and design: Dr. Larry Lands

Data collection: Farah Al-Huda with Dr. Larry Lands or Dr. Bashayer Al-Nuaimi as on-site physician

Data analysis and interpretation: Farah Al-Huda, Dr. Zoltan Hantos, Dr. Larry Lands

Thesis Draft: Farah Al-Huda

French Abstract translation: Georgia Limniatis

Draft Revision and Final Approval: Dr. Larry Lands

List of Tables

List of Figures

List of Abbreviations

AOS	Airwave Oscillometry System™
AX	reactance area below f_{res}
C_{CW}	chest wall compliance
CIM	Centre for Innovative Medicine
C_L	lung compliance
COH	coherence
COPD	chronic obstructive pulmonary disorder
COVID-19	Coronavirus-19 disease
C_{rs}	respiratory compliance
CV	coefficient of variation
E	lung elastic recoil
E_{RS}	European Respiratory Society
f	frequency
FEV1	forced expiratory volume in 1 second
FRC	functional residual capacity
f_{res}	resonant frequency
FVC	forced vital capacity
ICC	intraclass correlation coefficient
IOS	impulse oscillometry system
I_{rs}	inertance of the respiratory system
LoA	limits of agreement
LRTI	lower respiratory tract infection
MBW	multiple breath washout
MUHC	McGill University Health Centre
OSC	oscillometry
OVW	optimal ventilator waveforms
P_{abd}	abdominal pressure
P_{alv}	alveolar pressure
P_{atm}	atmospheric pressure
P_{CW}	transthoracic pressure
P_{di}	trans-diaphragmatic pressure
P_{el}	pressure due to lung elastic recoil
P_L	transpulmonary pressure
P_{pl}	pleural pressure
P_r	pressure due to lung tissue resistance
PRN	pseudorandom noise
P_{rs}	pressure exerted on the respiratory system
R-C-L	resistance–compliance–inertance
R_{aw}	resistance to airflow in airways
RDS	respiratory distress syndrome
R_{eE}	resistance at end-expiration
R_{eI}	resistance at end-inspiration
REM	rapid eye movement
R_I	resistance due to inertial forces

$R_{max,E}$	maximum resistance during expiration
$R_{max,I}$	maximum resistance during inspiration
R_{mean}	mean resistance during breathing cycle
$R_{min,E}$	minimum resistance during expiration
$R_{min,I}$	minimum resistance during inspiration
RR	respiratory rate
R_{rs}	respiratory resistance
R_t	lung & chest wall tissue resistance
RTC	rapid thoracic compression
R_{tCW}	chest wall tissue resistance
R_{tL}	lung tissue resistance
RV-RTC	raised volume-rapid thoracic compression
SD	standard deviation
SEM	standard error of measurement
SNR	signal-to-noise ratio
T_e	expiratory time
T_{tot}	total respiratory cycle time
TTN	transient tachypnea of the newborn
UAB	University of Alabama at Birmingham
V	volume
V'	flow
V''	volume acceleration
V_E	minute ventilation
V_T	tidal volume
X_C	compliance component of reactance
X_{eE}	reactance at end-expiration
X_{eI}	reactance at end-inspiration
X_I	inertial component of reactance
$X_{max,E}$	maximum reactance during expiration
$X_{max,I}$	maximum reactance during inspiration
X_{mean}	mean reactance during breathing cycle
$X_{min,E}$	minimum reactance during expiration
$X_{min,I}$	minimum reactance during inspiration
X_{rs}	respiratory reactance
Z_{in}	input impedance
Z_{rs}	respiratory impedance
Z_{uaw}	upper airway impedance
τ_{rs}	time constant of respiratory system

Chapter 1: Introduction

The physiological function of the respiratory system is to supply oxygen to tissues for cellular metabolism and expel carbon dioxide produced by tissues as metabolic waste. This chapter starts with a brief overview of the respiratory system, specifically the anatomical and functional divisions of the system, the sequence of events during one breathing cycle and the unique breathing mechanics of infants. The next section outlines three mechanical models used to study the lung: the linear single-compartment, viscoelastic tissue and constant-phase tissue models. Finally, the principles and parameters of oscillometry (OSC) are described, followed by a focus on the current gold standard OSC device, the Wave-tube Oscillometer, and the device to be validated, the tremoFlo® N-100 Airwave Oscillometry System™ (AOS).

1.1 The Respiratory System

The respiratory system is structurally organized into the upper and lower respiratory tract. The upper airways consist of the nose, mouth, nasal and oral cavities, pharynx and larynx, while the lower airways consist of the trachea, bronchi and bronchial tree. The lower respiratory tract is made up of 23 generations of branching airways. Based on function, the first 16 generations are classified as the conducting zone, since no gas exchange occurs. This anatomic dead space includes the trachea, bronchi, bronchioles and terminal bronchioles. Thereafter is the respiratory zone, where gas exchange occurs, made up of respiratory bronchioles and alveolar ducts and sacs[1].

Central, or proximal, airways are those larger than 2 mm and reside in the conducting zone. Small, or peripheral, airways of less than 2 mm diameter are thought to occur around the eighth generation and span both the conducting and respiratory zones[2]. As the airways extend distally into the lungs, the individual diameter of each airway decreases, while the total cross-sectional area increases causing a decrease in total resistance[3]. The resistance of peripheral airways is so much smaller than that of central airways that changes in resistance are difficult to detect. Thus, they are collectively known as the 'silent zone'[1]. Intrathoracic airways embedded within lung parenchyma are tethered by radial forces exerted by parenchymal tissues to keep them open at high lung volumes, decreasing resistance during lung inflation. At low lung volumes, the loss of tethering causes airway closure during lung deflation[1,3].

1.1.1 Respiratory Physiology

During the breathing cycle, the force of muscle contraction is translated into the pressure changes that drive airflow. It becomes evident when pressure, flow and volume are plotted against time for a single spontaneous breath (Fig. 1[1]).

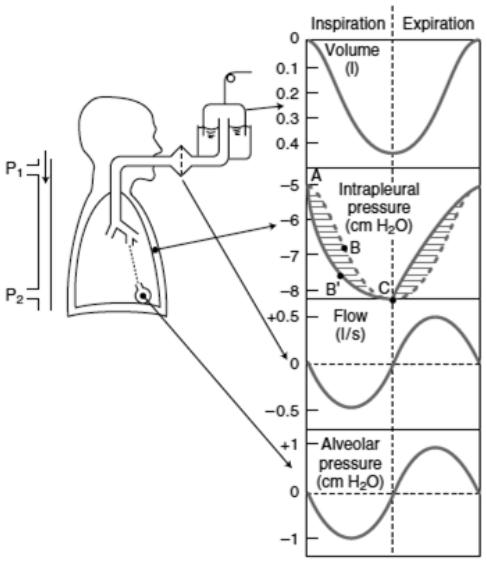

Figure 1. Pressure, flow and volume over time for one breathing cycle in a healthy adult

Before inspiration, with no net movement of air, alveolar pressure (P_{alv}) is in equilibrium with P_{atm}. The force of inspiratory muscle contraction generates negative pressure in the pleural space, causing the lungs and alveoli to expand, which decreases P_{alv} below P_{atm}. This pressure gradient then drives airflow from the atmosphere into alveoli. The amount by which P_{alv} drops below zero depends on airway resistance (R_{aw}). As air flows into the alveoli, P_{alv} starts to rise back up to zero, as it starts to equilibrate with P_{atm}. The smaller pressure gradient causes less air to flow into the alveoli until it eventually stops. The dashed lines in the figure reflect the static state in which pleural pressure (P_{pl}) is required to overcome the elastic recoil of the lung only. The solid lines reflect the dynamic state in which P_{pl} is required to overcome the elastic recoil of the lung (P_{el}) and lung tissue resistance (P_r)[1].

Normal expiration is passive because the elastic energy stored during inspiration dissipates to overcome expiratory frictional resistance. The muscles relax and the lungs deflate due to inward elastic recoil. Thoracic volume decreases, causing P_{alv} to rise above P_{atm}. This pressure gradient then drives air to leave the lungs. P_{pl} also rises (or becomes less negative) until it reaches a slightly negative resting value[1].

1.1.2 Respiratory Mechanics

The mechanics of breathing refers to the way in which the respiratory system moves air in and out of the lungs. The force of respiratory muscle contraction generates the pressure changes that drive air into the lungs. The diaphragm is the primary respiratory muscle, in addition to accessory muscles, like the intercostal and abdominal wall muscles. To move air into the lungs, it must overcome the mechanical forces of a) elastic recoil of lung, chest wall and abdominal tissue (proportional to volume), b) friction during airflow in the respiratory system (proportional to the rate of airflow) and c) inertia of the respiratory system (proportional to volume acceleration)[3]. Thus, the pressure exerted on the respiratory system (P_{rs}) is a function of changes in volume (V), flow (V') and volume acceleration (V") expressed as:

$$P_{rs} = f_1(V) + f_2(V') + f_3(V") \quad (1)$$

When the respiratory system acts in a linear fashion over a specific range of V, V' and V", Equation 1 can be rewritten as the linear equation of motion:

$$P_{rs} = (V - V_0)/C_{rs} + R_{rs}V' + I_{rs}V" \quad (2)$$

C_{rs} is respiratory compliance, which describes the respiratory system's elastic property, R_{rs} is respiratory resistance, describing the system's frictional property and I_{rs} is respiratory inertance, which describes the respiratory system's inertial property. V_0 is the volume at which elastic recoil pressure is zero[3].

In quiet breathing, the lung deflates during expiration due to its inward elastic recoil (E), which is the reciprocal of C_{rs}. As seen in Equation 2, C_{rs} is the relationship between volume and pressure, equivalent to the slope of a pressure-volume (PV) curve:

$$C_{rs} = \frac{1}{E} = \frac{\Delta V}{P_{rs}} \quad (3)$$

Structures with low compliance require larger pressure gradients for a given increase in volume, while those with high compliance require smaller pressure gradients for the same increase in volume.

Respiratory resistance expresses the relationship between driving pressure and flow:

$$R_{rs} = \frac{P_{rs}}{V'} \quad (4)$$

Structures with high resistance require larger pressure gradients for a given rate of airflow, while those with low resistance require smaller pressure gradients for the same rate of airflow.

Inertia refers to the tendency of structures at rest to remain at rest unless acted upon by an external force. Static air and tissues within the respiratory system need to be overcome by a pressure gradient to initiate acceleration.

Air is driven into each component of the respiratory system by different pressure gradients. In the airways, it is the difference between P_{alv} and P_{atm}. The driving pressure for lung tissue, known as transpulmonary pressure (P_L), is the pressure difference between P_{pl} and P_{alv}. The driving pressure for the chest wall, known as transthoracic pressure (P_{CW}), is the pressure difference between P_{atm} and P_{pl}[3]. Although traditionally, the term transpulmonary pressure (P_L) referred to the pressure difference across both, airways and lungs, the commonly used current definition referring to the pressure difference across the lungs only is used here.

1.1.3 Respiratory Physiology & Mechanics in Infants versus Adults

The differences in infant respiratory physiology compared with adults and their impact on respiratory mechanics are summarized in Table 1 at the end of this section[4], while those relevant to oscillometry are described below.

Respiratory compliance (C_{rs}) consists of lung (C_L) and chest wall (C_{CW}) compliance. In adults, the lungs and chest wall contribute equally to total compliance. However, infants have a C_{CW} that is four to five times higher than their C_L, as their cartilaginous ribs render the chest wall floppy[5]. Because the lung and chest wall work in tandem, they are summed in parallel:

$$\frac{1}{C_{rs}} = \frac{1}{C_L} + \frac{1}{C_{CW}} = \frac{1}{C_L} + \frac{1}{5C_L} = \frac{1}{6C_L} \quad (5)$$

Equation 5 shows that 83% of C_{rs} consists of C_L, while C_{CW} can be assumed to be negligible in infants[6], conferring a practical advantage since C_L is relatively easier to measure than C_{CW}[6]. In a young healthy newborn, a typical C_L measures 1.5 to 2.0 mL/cm H_2O/kg[7]. As an infant grows, the mass of elastic tissue in the lung increases, thereby increasing C_L[7], while C_{CW} decreases as the ribs ossify[4].

Compared to adults, infants have a much higher metabolic rate that requires higher minute ventilation ($V_E = RR \times V_T$)[8]. V_E can be increased by increasing respiratory rate (RR) or tidal volume (V_T). To increase V_T, a more negative P_{pl} needs to be generated, so the diaphragm contracts to increase trans-diaphragmatic pressure (P_{di}) and abdominal pressure (P_{abd})[8]. This causes the abdomen and lower rib cage to expand. However, the highly compliant chest wall collapses under the large negative P_{pl}, resulting in paradoxical inward movement of the upper rib cage, which sets a functional limit to the maximum V_T possible[8]. Since the highly compliant chest wall prevents infants from increasing V_T, they opt to breathe at a higher respiratory rate, instead, to meet their metabolic demands[8]. Normally, the intercostal muscles compensate for the paradoxical movement, but they are inefficient in infants because their ribs are aligned more horizontally, ultimately wasting the energy from diaphragm contraction on the chest wall distortion[4].

In adults, resting lung volume or functional residual capacity (FRC) is determined by the static balance between the inward elastic recoil pressure of the lung and the outward elastic recoil pressure of the chest wall. In infants, this equilibrium point is lower[4,9]. Low FRC results in decreased O_2 reserves in the lungs at end-expiration, leading to rapid O_2 desaturation. Moreover, the lower C_L relative to C_{CW}, causes the closing volume to be greater than FRC in infants, such that the small airways are at risk of collapse during normal tidal breathing[4,9]. Infants overcome this using an adaptive mechanism that actively increases and maintains a dynamically elevated FRC, also known as dynamic hyperinflation. Generally, hyperinflation is favoured by increasing V_T, shortening expiratory time (T_e) and prolonging the time constant to empty the respiratory system ($\tau_{rs} = R \times C$)[4,8,9]. The high infant respiratory rate shortens T_e relative to τ_{rs}, maintaining the elevated FRC. Prolonging τ_{rs} causes the next inspiration to begin before the previous expiration is complete, thereby increasing FRC. This is achieved by activating the diaphragm and intercostals after inspiration to delay passive recoil of the lungs and chest wall, as well as adducting the vocal cords during expiration to increase airway resistance, known as expiratory braking[4,8,9].

Respiratory resistance consists of non-elastic properties of the system, specifically frictional resistance to airflow in airways (R_{aw}), frictional resistance of moving tissues in the lungs (R_{tL}) and chest wall (R_{tCW}) and inertial forces (R_I). In a spontaneously breathing adult, overall R_{rs} consists of about 80% R_{aw}, 19% R_t, with equal contributions from the lungs and chest wall, and 1% resistance due to inertia (considered negligible in tidal breathing and the linear model of the respiratory system)[7].

Poiseuille's Law states that the pressure (ΔP) required to achieve a specific flowrate (V') of a gas with η viscosity through a rigid, smooth cylindrical tube of length L and radius r can be calculated using:

$$\Delta P = \frac{V\prime 8\eta L}{\pi r^4} \quad (6)$$

When airflow is laminar and airways act like rigid, smooth cylindrical tubes, R_{aw} can be calculated according to this Law based on the pressure drop from one end of a tube to the other that drives a specific flowrate. Thus, the above equation expressed in terms of resistance, like in Equation 4, is:

$$R_{aw} = \frac{\Delta P}{V\prime} = \frac{8\eta L}{\pi r^4} \quad (7)$$

The driving pressure used for ΔP in this case would be the pressure difference between P_{alv} and P_{atm}. Evident in Equation 7 is the significant role of radius in determining resistance. The airway lumen of a newborn is about half of that of an adult, making infant R_{aw} 16 times higher than an adult (20 to 40 cm H_2O/L/s vs. 1 to 2 cm H_2O/L/s, respectively)[7]. Consequently, even a small obstruction in an infant's airway leads to an exponential increase in resistance to airflow. Moreover, Equation 7 assumes laminar flow, which occurs in small airways. The larger the airway, the higher the velocity and turbulence of airflow. Airflow also becomes turbulent in situations like when an infant cries, increasing R_{aw} 32-fold[10].

To calculate R_{tL}, the driving pressure used for ΔP is the pressure difference between P_{pl} and P_{alv}, while R_{tCW} uses the pressure difference between P_{atm} and P_{pl}. Thus far, the simple linear model has been used to explain mechanics. However, when it comes to R_t, this model no longer holds, as it ignores the time- or frequency-dependence of respiratory tissue, that is accounted for in the viscoelastic tissue model.

Table 1. Main differences between respiratory physiology of infants vs. adults

Difference in Infants	**Physiology/Mechanics**
rapid O_2 desaturation	increased rate of O_2 consumption
	smaller O_2 reserve relative to body size
increased risk of apneas	immature respiratory control
increased airway resistance	smaller airway size
	increased risk of airway collapse due to increased airway compliance
increased risk of losing FRC	decreased lung compliance
	closing pressure near or below FRC
	active, dynamic FRC elevation
decreased efficiency of respiratory muscles	fewer type I (slow endurance) muscle fibres
	increased chest wall compliance
	ribs aligned more horizontally

1.2 Mechanical Models of the Respiratory System

Different models have been proposed to illustrate how the mechanical properties of respiratory structures perform their designated function.

1.2.1 Single-Compartment Linear Model

The simplest way to model the respiratory system is the single-compartment linear model. It can be depicted as two telescoping canisters connected by a spring that is attached to their horizontal bars (Fig. 2[11]). Air flows (V') through a column, representing airways, to encounter a constant frictional resistance (R_{aw}), before entering a compartment of volume, V, representing the lung. Hooke's Law states that the deformation of an elastic object (ΔV), like a spring or lung, is proportional to the pressure required to produce that deformation (P_{el}). This proportionality is reflected in the spring constant, k, of the spring, which represents the static elastance of the lung. Thus, the pressure change (P_{rs}) required for inflation, resulting in the movement of the bars, is the sum of the pressures required to overcome static elastic force (P_{el}) of the lung and airway resistance (P_r)[11]. This can be expressed using the linear equation of motion from Equation 2 as:

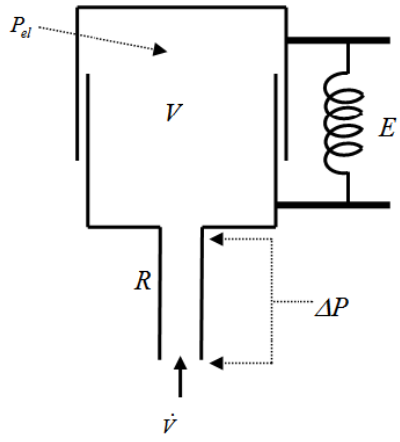

Figure 2. Single-compartment linear model. ΔP = pressure to overcome airway resistance (P_r)

$$P_{rs} = P_{el} + P_r = \frac{\Delta V}{C_{rs}} + R_{aw}V' \qquad (8)$$

However, this model ignores the dynamic (time-dependent) properties of tissue resistance and elastance, as well as inertial forces (R_I).

1.2.2 Viscoelastic Tissue Model

The viscoelastic model accounts for the dynamic properties of viscoelastic respiratory tissues by adding a second spring (E_2) in series with a dashpot (R_2) (Fig. 3[12]). Together, they act like a shock absorber to slow down the motion of the second spring's piston as it encounters the frictional element of the dashpot. This modification allows the model to reflect the time-dependent element of tissue elastance (E_2) via the second spring and the viscous element of tissue resistance (R_2) via the dashpot[12]. High frequency oscillations move the horizontal bars further apart and closer together in a rapid, rhythmic motion. This causes both springs to undergo immediate compression-decompression, but the movement of the piston through the dashpot takes longer to adjust to the abrupt volume changes.

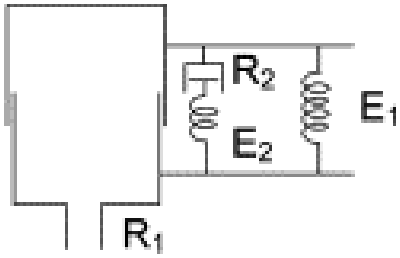

Figure 3. Viscoelastic model. R_1: frictional resistance to airflow through airways (R_{aw}), R_2: frictional resistance of moving respiratory tissue (R_t); E_1: static lung elastance, E_2: viscoelastic lung elastance

Physiologically, during high respiratory rates, tissues are not given enough time to adapt to the quick stress-relaxation cycles and contribute a smaller proportion of R_t to R_{rs}, compared to R_{aw}. Although attempts to quantify the contribution of each component have yielded mixed results[13–16], the current generally accepted value

for R_t is 20% in humans[17]. Part of the variability is due to the complex physiological mechanisms that cause both airway and tissue resistance to depend on the frequency of ventilation, which this model fails to capture[17].

1.2.3 Constant-Phase Tissue Model

The constant-phase model[18] is able to distinguish between the frequency dependence of airway resistance and that of viscoelastic tissue (Fig. 4[11]). Mechanical impedance (Z_{rs}) is a measure of the extent to which a mechanical system, like the respiratory system, resists motion when subjected to mechanical oscillations. It can be expressed as a function of frequency (f):

$$Z_{rs}(f) = R_{aw} + j2\pi f \cdot I_{aw} + \frac{G - jH}{2\pi f^{\alpha}} \quad (9)$$

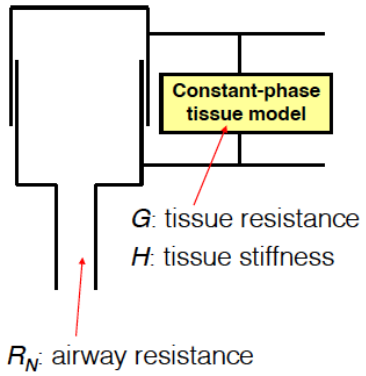

Figure 4. Constant-phase model. R_N = airway resistance (R_{aw})

R_{aw} represents frictional resistance to airflow in airways, j is an imaginary number ($\sqrt{-1}$), I_{aw} represents inertia of the air column within central airways, G stands for tissue damping that accounts for the viscous property of tissues contributing to resistance (R_t), H represents the elastic or compliant property of tissues (C_{rs}) and α is a complex function of G and H that is usually equal to slightly less than one[11,12,17,19].

The springs and dashpot are replaced by a constant-phase tissue unit characterized by G, related to energy dissipation as heat when respiratory tissues are oscillated, and H, related to energy storage as elastic energy[11]. Accounting for the frequency dependence of tissues confers the ability to somewhat quantify R_t by showing how it decreases as frequency increases ($R_t = \frac{G}{2\pi f^{\alpha}}$)[17]. This model elegantly partitions the airway parameters of R_{aw} and I_{aw} from tissue parameters, G and H[20]. It also provides a significantly improved model that fits decades of oscillometry data[17].

1.3 Oscillometry

Pioneered by Dubois et al.[21], oscillometry (OSC; also known as forced oscillation technique) provides information about lung mechanics by applying oscillations at the airway opening or body surface. It was not widely used at the time, as it required specialized equipment and difficult, time-consuming calculations to resolve respiratory impedance (Z_{rs}) from the pressure (P) and flow (V') signals[19]. With the advent of technology and faster digital processing of more complex signals, its use has gained popularity. OSC is especially useful for measuring lung function in infants because it is non-invasive and requires minimal subject cooperation, as testing can be conducted during quiet breathing.

1.3.1 Principles of Oscillometry

Oscillometry (OSC) measures the amount of pressure generated by the respiratory system to move a given volume of air into and out of the lung[19]. This allows the direct assessment of key mechanical parameters: R_{rs}, C_{rs} and I_{rs}. Mechanical perturbations from an external source (a loudspeaker in Fig. 5[22]) are superimposed onto spontaneous breathing over a short period of time, typically a minute or two. These low-amplitude oscillatory flow waves are generated at a higher frequency than normal breathing frequency to avoid interference. To measure input impedance (Z_{in}), oscillatory changes in pressure (P) and flow (V') signals are recorded at the airway opening by pressure transducers and a pneumotach, respectively.

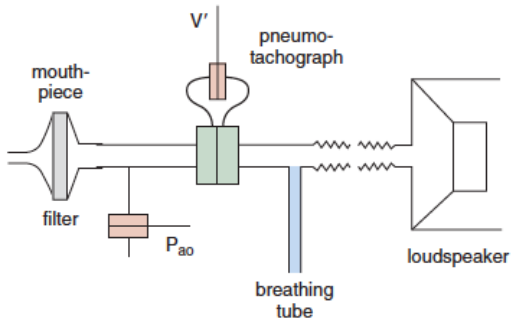

Figure 5. A conventional oscillometry setup

A pneumotach contains an element of known resistance, either a honeycomb arrangement of conduits (Fleish-type) or a mesh screen (Lilly-type) to decrease turbulence. As air flows over this resistance, instantaneous pressure is measured on either side using differential pressure transducers. The linear relationship between flow and pressure in laminar flow can then be used to calculate flow based on the pressure drop across the resistive element[23]: $V' = \frac{p_2 - p_1}{R}$.

The subject breathes through the mouthpiece equipped with an antimicrobial filter. The recorded P and V' signals contain frequencies of both, normal breathing and the superimposed oscillations. The breathing components are filtered out to leave behind only the oscillation component[19]. This waveform contains the mechanical response of the respiratory system[19]. Filtering signals also eliminates noise from cardiogenic oscillations, which are small mechanical lung deformations caused by each heartbeat, prominent at 1 to 4 Hz[19].

Recall that the equation of motion from Section 1.1.2 applies to the respiratory system when it acts in a linear fashion. Assuming the lung is a linear dynamic system, for a given volume of air to enter the lung, the pressure it needs to generate as a function of time is:

$$\mathrm{P}(t) = \frac{V(t)}{C_{rs}} + R_{rs}V'(t) + I_{rs}V"(t) \qquad (2)$$

The mechanical input impedance (Z_{rs}) is expressed as the ratio of the Fourier transform of P(t) to V'(t) in terms of frequency (f)[11]:

$$Z_{rs}(f) = \frac{P(f)}{V'(f)} \qquad (10)$$

With V as the integral of V' and V" as the derivative of V'[24], the Fourier transform of Equation 2 gives[11]:

$$P(f) = -\frac{j}{2\pi f}\frac{V'(f)}{C_{rs}} + R_{rs}V'(f) + j2\pi f \cdot I_{aw}V'(f)$$

$$= V'(f)\left[R_{rs} + j\left(2\pi f \cdot I_{aw} - \frac{1}{2\pi f C_{rs}}\right)\right] \quad (11)$$

$$Z_{rs}(f) = \frac{P(f)}{V'(f)} = \left[R_{rs} + j\left(2\pi f \cdot I_{aw} - \frac{1}{2\pi f C_{rs}}\right)\right]$$

Thus, Equation 11 shows that impedance is a complex function of frequency that includes all the mechanical forces hindering airflow into and out of the respiratory system, specifically a) compliance (blue), b) resistance (red) and c) inertance (green). It is usually simplified to show impedance (Z_{rs}) as the vector sum of effective resistance (R_{rs}) and effective reactance (X_{rs})[11,24]:

$$Z_{rs} = R_{rs} + jX_{rs} \quad (12)$$

R_{rs} reflects the real component of Z_{rs}, where pressure signals are in phase with flow signals[25]. X_{rs} is the sum of the compliant (X_C) and inertial (X_I) components of reactance[24]:

$$X_C = -\frac{1}{2\pi f C_{rs}} \quad (13)$$

$$X_I = 2nfI \quad (14)$$

X_{rs} reflects the imaginary component of Z_{rs}, where pressure is out of phase with flow, but in phase with volume[25]. When volume changes at low frequencies, the elastic tissues cause pressure changes to lag behind flow changes, making reactance negative. Thus, more negative (decreased) reactance reflects increased elastance or decreased dynamic compliance, denoting stiffer tissues (Fig. 6[25]). The term elastance is analogous to stiffness in the mechanical domain and is the inverse of compliance in the fluid flow domain. As mentioned in section 1.1.2, a pressure gradient needs to overcome the inertia of air and tissues to initiate acceleration. At high frequencies, inertance causes pressure changes to lead flow changes, making reactance positive.

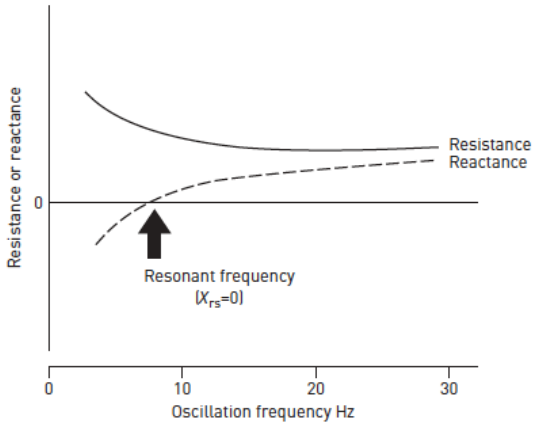

Figure 6. Resistance and reactance curves generated by oscillometry

Resonant frequency (f_{res}) is the frequency at which the compliance (X_C) and inertial (X_I) contributions to X_{rs} are equal in magnitude but opposite in sign, cancelling each other[24]. Thus, at f_{res}, when reactance is zero, pressure changes depend only on flow resistance and flow rate[24,25]. This frequency has a zero phase angle between pressure and flow[24] and can be calculated by[26]:

$$f_{res} = \frac{1}{2\pi\sqrt{CI}} \quad (15)$$

Thus, Z_{rs} conveys the spectral, or frequency domain, relationship between pressure and airflow to provide a global measure of resistive, elastic and inertial forces throughout the respiratory system.

1.3.2 Interpretation of Oscillometry in Health

Using OSC at different frequencies provides different insights into the respiratory mechanics of a healthy adult. The standard frequency range used in a typical oscillometer is 5 to 40 Hz[19], as Z_{rs} can be described by a simple resistance-compliance-inertance (R-C-L) model within this range[27].

In a healthy adult, resistance below 5 Hz has a negative frequency dependence. As frequency decreases, R_{rs} increases rapidly, reflecting both airway resistance (R_{aw}) and tissue resistance (R_t). Above 5 Hz, as frequency increases, R_t diminishes, thus R_{rs} reflects only R_{aw} and is independent of frequency over the standard OSC range[19,25].

As frequency decreases below 5 Hz, reactance becomes more negative to reflect compliance of respiratory tissue (C_{rs}) only[25]. Above 5 Hz, the X_{rs} curve reflects both tissue compliance (C_{rs}) and the compressibility of air in the airways and alveoli[25]. With further increases in frequency, C_{rs} diminishes, making X_{rs} less negative (increase) until it reaches zero at f_{res}. In a healthy adult, f_{res} typically occurs at around 8 to 12 Hz[28]. At this point, impedance reflects true resistance, since there is zero contribution from reactance[21,24]. As frequency increases beyond f_{res}, X_{rs} increases, mostly reflecting inertance of the air column in central airways, with a small contribution from tissues[25]. The latter becomes significant at higher oscillation frequencies[25].

Impedance increases with decreasing age due to the smaller lung sizes of children and infants, shifting the R_{rs} and X_{rs} spectra of healthy children and infants to the right. With decreasing age, the negative frequency dependence of R_{rs} becomes more evident[29–33], such that healthy children demonstrate this relationship well beyond 5 Hz and into the standard OSC frequency range[25]. Also with decreasing age, X_{rs} increases, shifting f_{res} to over 20 Hz[34] and 30 Hz[25] in children and infants, respectively.

Infant impedance at low frequencies of 1 to 2 Hz contains information on the resistance and compliance of lung and chest wall tissue[35]. The chest wall tissue contribution to Z_{rs} decreases with increasing frequency and decreasing age[25,36]. Z_{rs} over the frequency range of 5 to 15 Hz reflects R_{aw}[25], while Z_{rs} over 50 Hz reflects the acoustic wave properties of central airways and airway wall compliance[9,25].

1.3.3 Clinical Interpretation of Oscillometry

Adults with obstructive lung disease, such as asthma, have narrower airways, which increases resistance (R_{rs}), and less compliant or stiffer lungs, which decreases reactance (X_{rs}) to more negative values[19]. Airflow obstruction also increases f_{res}[37], causing effective resistance at f_{res} to contain an in-phase portion of reactance in addition to true resistance[24]. The reactance area below f_{res} (AX), which is the integral of the area of the reactance curve from the lowest frequency to f_{res}, is also increased in asthma compared

with healthy adult controls[19,38,39]. However, the ability of OSC to distinguish between health and asthma in children has shown mixed results[40–43].

In obstructive lung disease, not all airways narrow to the same degree (R_{aw}), or even narrow at all, nor do all regions of the lungs become stiffer (C_{rs}). This heterogenous distribution of disease contributes further to the frequency dependence of respiratory impedance seen in health, amplifying them at low frequencies and displaying this dependence well into the standard OSC frequency range.

The frequency dependence of R_{rs} may be expressed as the difference between R_{rs} values at a low and high frequency, usually $R_{rs\ 5\text{-}20}$[22,25,37]. In the past, the relationship was attributed to heterogeneous narrowing mainly in the small airways[37]. However, frequency dependence is also influenced by other factors, like heterogeneous narrowing in central airways and viscoelastic tissue resistance (R_t)[22,25,37]. Moreover, heterogenous distribution of disease affects not only the airways, but also lung tissue. This results in different regions of the lungs having different time constants ($\tau_{rs} = R \times C$)[4,8,9,22,25]. Mixed τ_{rs} make effective reactance, and thus dynamic compliance, sensitive to frequency, with increasing heterogeneity at any given frequency causing a decrease in reactance or dynamic compliance[25].

The final contributing mechanism to the frequency dependence of impedance is the upper airway shunt. It occurs when some of the generated oscillatory flow is diverted or 'shunted' to the more compliant structures of the upper airways, like the pharynx and cheeks, decreasing flow to the lower respiratory tract[19,44]. This loss in oscillatory flow leads to an underestimation of Z_{rs}, especially at higher frequencies[34]. In cases of high impedance, such as those of infants, this airway artefact also overestimates the frequency dependence of R_{rs} and shifts X_{rs} to the right, increasing f_{res}[34]. Although cheek support is thought to partially correct for this upper airway artefact in adults and children, it requires subject comprehension not feasible in infants[45].

The head generator technique (Fig. 7[45]) was used to minimize the influence of the upper airways by generating oscillations around the surface of the subject's head to measure transfer impedance, instead of at the airway opening, which measures input impedance[46]. Doing so decreased transmural pressure across the upper airways and was found to completely eliminate the upper airway shunt in adults[46]. However, in infants, the assumption of zero upper airway wall motion does not hold, as infants are habitual nose breathers, which induces a driving pressure that causes upper airway wall movement[45]. Yet, using the head generator technique, in addition to directly estimating upper airway impedance (Z_{uaw}), based on previously measured nasal impedance, showed that the method corrected for the upper airway shunt,

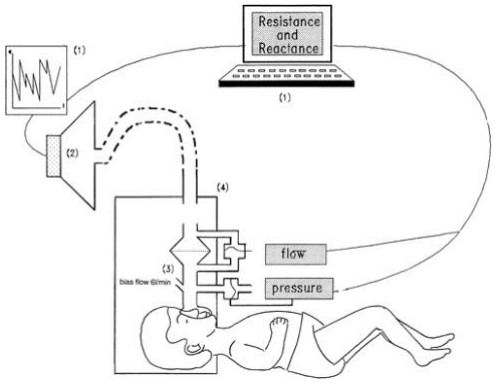

Figure 7. Setup of head generator technique to minimize upper airway shunt

shifting the X_{rs} curve back to the left and decreasing f_{res} in infants[34,45]. The authors did concede that the setup required was too impractical for routine use.

Since infants are habitual nose breathers, lung function measurements need a facemask. With nasal resistance contributing up to 50% of resistance to airflow in airways (R_{aw})[9] and air within the mask adding to the equipment dead space as parallel shunt impedance, impedance measurements are significantly affected[9]. The consequences are compounded in the presence of heterogeneous ventilation due to airway obstruction because the detection of small changes in respiratory mechanics is hindered[25]. It may explain one of the reasons for the availability of a wide variety of oscillometers for older children and adults, who can breathe orally, but no commercially available devices for infants.

1.4 OSC Devices

1.4.1 Development of OSC Devices

As technology advanced, the devices used for oscillometry became more sophisticated using more complex waveforms (Fig. 8[47]). Early oscillometers used a simple single-frequency sinusoidal wave, which yielded a high signal-to-noise ratio (SNR) due to the signal power being concentrated at one frequency[19]. However, after taking painstaking measurements at many different frequencies, it was observed that changes in R_{rs} in the frequency domain were different in healthy adults compared with those with chronic obstructive pulmonary disorder (COPD)[48], sparking interest in Z_{rs} spectra. The next generation of oscillometers used a continuous multi-frequency signal composed of random noise ranging from 3 to 45 Hz[19,47].

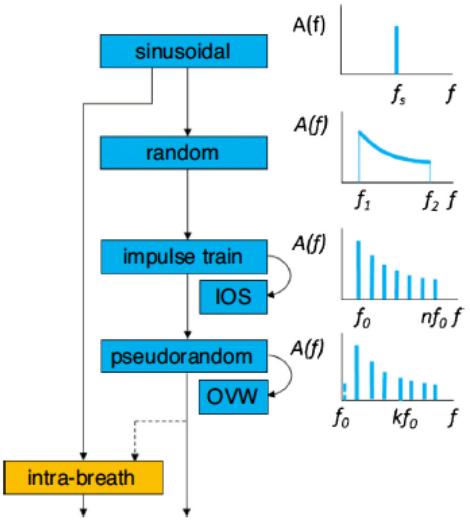

Figure 8. Development of OSC devices with progressively more sophisticated waveforms

Some modern oscillometers, like impulse oscillometry systems (IOS), use harmonic impulse trains composed of recurring signals over multiple frequencies (2-32 Hz) at discrete time intervals[19,47]. The drawback of using harmonics of a fundamental frequency is noise contamination of the waveform when the respiratory system acts in a non-linear manner, such as during severe airflow obstruction[25].

The pseudorandom noise (PRN) waveform is another type of signal commonly used in modern devices. The sinusoidal oscillatory flow signals generated consist of mutually prime frequencies, which minimises noise contamination from nonlinearities[25,47]. The composite signal includes frequencies corresponding to prime numbers of a specific fundamental frequency, but not the fundamental frequency itself[25]. Although signal filtering eliminates breathing components, noise from breathing frequencies and

its harmonics may still remain at low frequencies, especially at the high respiratory rates of infants[25,47]. This is avoided by optimizing the signal so that the signal power at each frequency is the same, regardless of the noise power, and by minimizing peak-to-peak amplitude[19,25,47]. Noise from breathing components can also be eliminated by using a modified ventilator to ventilate the subject, at the same time as optimal ventilator waveforms (OVW) deliver PRN signals at low frequencies ranging from 0.15 to 8 Hz[19].

1.4.2 Wave-tube Oscillometer

The Wave-tube Oscillometer (University of Szeged, Szeged, Hungary) was developed to measure lung function in infants during spontaneous breathing in a non-invasive manner that does not require sedation (Fig. 9)[49]. It is the current gold standard infant OSC device approved for research[26,49–52].

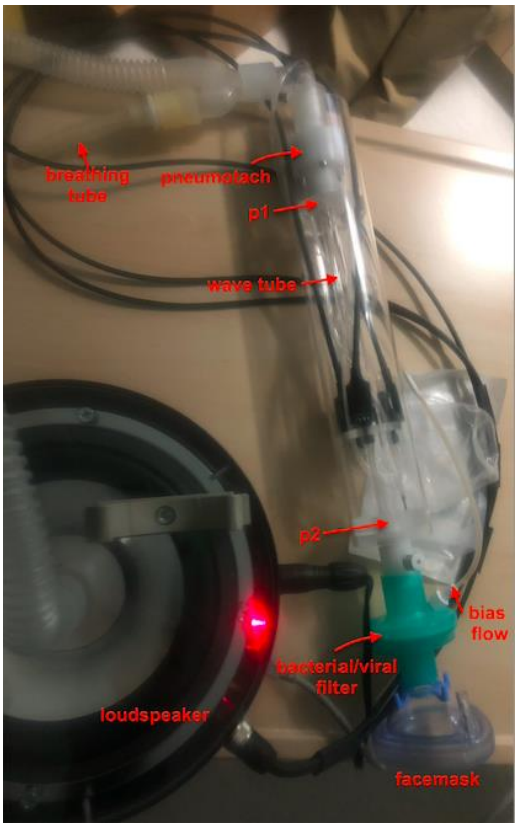

Figure 9. Wave-tube Oscillometer with loudspeaker (L) and flow head (R)

The wave-tube consists of a loudspeaker that provides mechanical perturbations to generate the oscillatory flow signals, which are superimposed onto the tidal breathing of a sleeping infant. The device uses a modified forced oscillation technique that circumvents the technical challenges of maintaining high signal-to-noise ratio (SNR) in the presence of the elevated nasal resistance, impedance and respiratory rate of infants.

In adults, the typical breathing rate of 12 to 16 breaths per minute is equivalent to a breathing frequency of 0.1 to 0.3 Hz, with harmonics that extend to 3 to 10 Hz[19]. Infant respiratory rates are typically higher at 60 breaths per minute, equivalent to a breathing frequency of 1 Hz, with harmonics that extend even further into the typical OSC frequency range than adults[19]. Consequently, flow signals measured by pneumotaches in infants get contaminated with significant noise from breathing components, which reduces SNR and precision.

The modified technique (Fig. 10[22]) uses a long, rigid tube, instead of a pneumotach, and measures the ratio of inlet to outlet pressures, instead of pressure and flow signals[53]. Impedance values obtained with the classic (Fig.5[22]) and modified techniques were found to be similar, with the modified technique yielding

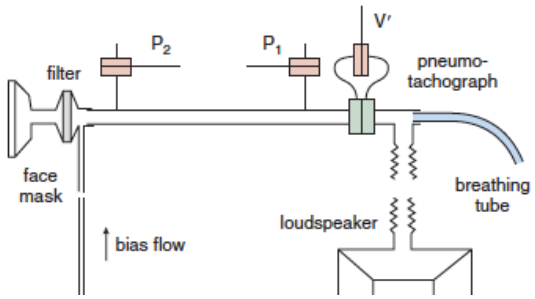

Figure 10. Modified oscillometry setup in wave-tube

more precise values in patients with airway obstruction[53], who also have high impedance like infants. The issue of significant flow-dependent changes due to nasal breathing[54] is bypassed by measuring inlet and outlet pressure ratios, eliminating the need to measure flow[53].

The calibration factor of tube impedance is based on the physical geometry of the tube, with the mechanical impedance of the respiratory system measured as load impedance on the tube[12,55]. The impedance of the filter-mask assembly (FMA) can also be precisely calculated by treating it as an arrangement of series and parallel impedances that are removed from the infant[49]. A Fleish-type pneumotach within the flow head only records the breathing flow signal, which is then filtered out. Although replacing the pneumotach from the classic technique with a tube introduces additional equipment dead space, it is easily flushed out by adding a bias flow of air near the mask that is set to approximately equal to the minute ventilation of the infant. The bias flow, attached to one side of an antimicrobial filter, flushes equipment dead space, while the subject breathes through the facemask on the other side.

The wave-tube was first used to test 34 healthy, term neonates on the first three days of life[49]. The authors found that obtaining non-invasive measurements of Z_{rs} during natural sleep in neonates was highly feasible (79% success)[49]. The wave-tube was included in multiple studies from the South African Drakenstein Child Health birth cohort followed from 2012 to 2015[26,50–52]. The goal was to investigate the epidemiology, etiology and risk factors for childhood lower respiratory tract infections (LRTIs).

The first study assessed the effect of various prenatal factors on lung function using the multi-frequency signal at 8 to 48 Hz of the wave-tube[26]. Measurements were made in 164 sleeping infants without sedation at 6 to 10 weeks old (93% success). It found that the wave-tube had sufficient sensitivity to demonstrate the effects of infant sex and exposure to tobacco smoke on respiratory mechanics in healthy infants.

The second study sought to establish reference lung function equations for healthy African infants using various techniques: tidal breath analysis, exhaled nitric oxide, multiple breath washout (MBW) and OSC[52]. Acceptable and repeatable measures were made with the wave-tube in 293 sleeping infants without sedation at 5 to 11 weeks old (88% success). The European equations were inadequate in predicting the South African values, so population-specific reference equations were developed.

A third study aimed to identify early life determinants of infant lung function using tidal breath analysis, MBW and OSC[51]. The wave-tube provided values in 508 sleeping infants without sedation at 6 to 10 weeks old (79% success). Several factors associated with altered early lung function were identified by

the techniques, including infant weight at the time of testing and sex, maternal smoking and HIV status, as well as household benzene. The wave-tube specifically detected higher R_{rs} and lower C_{rs} in male infants compared with females, while lower birth weight and gestational age were associated with lower C_{rs}.

The fourth study examined whether lung function indices from intra-breath analysis could identify healthy infants at risk of LRTI in the first year of life[50]. Wave-tube measurements were made using a mono-frequency signal at 16 Hz in 719 sleeping infants without sedation at 6 weeks old (78% success). Volume dependence of R_{rs} and X_{rs} were associated with subsequent LRTI, with a stronger predictive value if the LRTI was recurrent, associated with wheeze or required hospitalization. This study showed that intra-breath analysis can identify healthy infants who are at risk of developing LRTI, wheezing or severe illness at the age of one, creating the potential for monitoring and early intervention.

Respiratory resistance and reactance depend on lung volume. R_{rs} has an inverse relationship with the communicating lung volume, or the lung volume in communication with airway opening, such that R_{rs} increases significantly at low lung volumes. This relationship is amplified in preschool-aged children with airway obstruction[37,56]. X_{rs} is more sensitive to volume changes, decreasing suddenly and rapidly at low lung volumes due to airway closure[37]. As mentioned in section 1.1, radial forces from parenchymal tissues tether intrathoracic airways to keep them open at the high lung volumes of lung inflation, or inspiration, and the loss of tethering leads to airway closure at the low lung volumes of lung deflation, or expiration[1,3].

Intra-breath tracking at a single frequency allows closer examination of inspiration and expiration and the resulting changes in impedance. Changes in X_{rs} are especially useful to detect expiratory flow limitation and was found to discern healthy preschoolers from those with recurrent wheeze[37,57].

Despite providing insights from intra-breath analysis and being the current gold standard OSC device for infants, the wave-tube has thus far been limited to use in research settings. It has yet to be commercially developed, perhaps due to its complex computational requirements and difficulty related to use in routine clinical care.

1.4.3 tremoFlo® Airwave Oscillometry System™ (AOS)

Figure 11. tremoFlo® C-100 cradle and handheld unit with filter attached

The tremoFlo® C-100 Airwave Oscillometry System™ (THORASYS Thoracic Medical Systems Inc., Montreal, Canada) is a commercially available oscillometer suitable for use in adult and pediatric populations starting at two years old (Fig. 11[58]). Subjects are asked to support their cheeks to reduce shunt compliance, while wearing nose clips to ensure oral breathing through the filter. The device contains a patented vibrating mesh that provides mechanical perturbations to generate the oscillatory flow

signals superimposed onto the tidal breathing of awake subjects (Fig. 12[58]). The mesh is moved by the magnetic flux created by an electromagnetic voice coil[58].

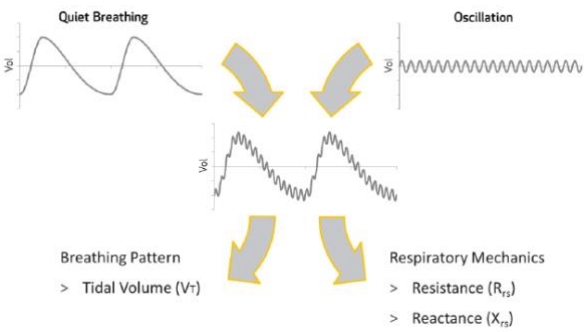

Figure 12. Oscillatory flow waves are superimposed onto the quiet breathing of subjects

Impedance is calculated using the pressure recorded at pressure port p2. Flow is calculated based on the differential pressure recorded by the pneumotach across ports p1 and p2 situated across a mesh screen with a known resistance. The total resistance to breathing is the sum of the resistances of the vibrating mesh, pneumotach and filter. The waveforms used are non-harmonic multi-frequency composite Airwave™ ranging from 5 to 37 Hz for adults and 7 to 41 Hz for children[59].

A research team at the University of Alabama at Birmingham (UAB) slightly modified this device by adding a 3D printed adaptor customized to fit an infant filter and mask, instead of the filter shown in Figure 11 (N. Restrepo, MEng, Research & Development Associate at THORASYS, e-mail communication, February 2022). The factory calibration was modified to account for the shunt impedance of this new filter, while the mask was considered a static part of the respiratory system[60]. The factory calibration was verified daily by measuring a test load with a known impedance of 2 cm $H_2O/L/s$[60]. The standard tremoFlo® software supplied by the manufacturer was used with no modifications[60].

The study tested 138 neonates without sedation on the first three days of life to derive OSC reference norms for healthy, term neonates[60]. They found that obtaining non-invasive measurements of Z_{rs} during natural sleep was feasible using the modified tremoFlo® C-100 (86% success)[60]. They also evaluated 17 neonates with transient tachypnea of the newborn (TTN), a common respiratory illness that usually resolves on its own (100% success). The authors found that the AOS™ could distinguish between health and disease, with TTN neonates presenting with higher R_{rs} at 13 Hz and lower X_{rs} at 17 to 37 Hz[60]. Mean resistance values were reported to be similar to those made by the wave-tube on the first three days of life[49], although it was acknowledged that the total tidal volume of the infant was not captured, as the dead space of the filter and mask were not flushed by a bias flow. Mean resistance was lower than those reported by Gray et al.[26], who tested slightly older infants aged 6 to 10 weeks.

Another study used the same device to compare 118 healthy term infants with 72 preterm infants (93% success)[61]. Preterm infants were found to have higher R_{rs} and lower X_{rs} compared with healthy infants. Moreover, the modified AOS™ was able to distinguish between preterm infants with and without respiratory distress syndrome (RDS), with the latter demonstrating lower X_{rs} than the former.

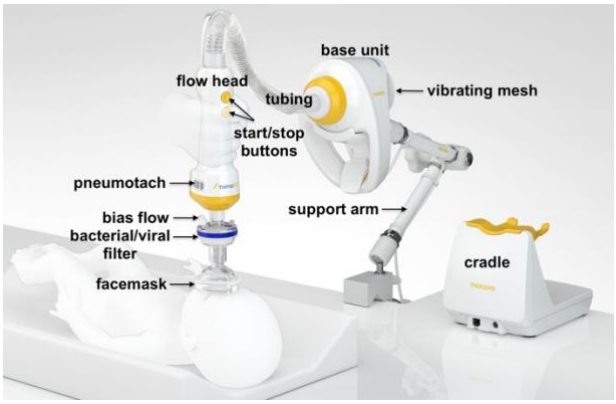

Figure 13. tremoFlo® N-100 Airwave Oscillometry System™, designed for infants below the age of two

However, the research team noted that vibrations generated by the device disrupted the infant's sleep and did not meet accuracy standards at the characteristic high impedance of infants. Based on this feedback, the manufacturer developed a new model called the tremoFlo® N-100 Airwave Oscillometry System™ (Fig. 13[58]). To keep the vibrations of the oscillator away from the sleeping infant, the redesign introduced an external flow head that is connected to the base unit by an adaptor located on the end of flexible tubing. The pneumotach, now equipped with a higher internal resistance, was relocated to this flow head, designed to fit a standard 15-mm antimicrobial filter for infants. It also has buttons to start and stop recording measurements, making it easier for the operator to start the test as soon as the facemask makes a seal covering the infant's nose and mouth. The former handheld unit, now called the base unit, can remain on the cradle or be attached to the bedside with an adjustable support arm.

A new waveform was developed to generate oscillatory flow waves with a higher amplitude. To increase accuracy of measurements made by the sensors at higher impedance, the gain for each sensor was modified and new test loads were used with a known impedance of 25 and 90 cm H_2O/L/s, including the filter (Gibeck Humid Vent filter model 19502). The UAB team is currently using this device to verify its feasibility and whether it can differentiate between health and disease in neonates.

Until now, there have been no studies comparing the tremoFlo® N-100 with the wave-tube, the current gold standard OSC device for infants. If values obtained by the tremoFlo® N-100 show sufficient reliability and agreement with those from the wave-tube, it would validate the N-100, providing a device with improved patient comfort and measurement accuracy for routine clinical use.

Chapter 2: Thesis

In the first few years of life, the respiratory system is exceptionally vulnerable to disease[22]. It is now known that lung function tracks throughout life, such that early abnormalities can predict long-term dysfunction[62,63]. The origins of chronic adult respiratory diseases, like asthma and COPD, have been traced back to early infancy[62,63]. Detection of lung function irregularities at a younger age would not only allow earlier intervention, but also enable continuous monitoring of the condition and response to treatment. Using lung function as a clinical outcome would help determine drug efficacy, thereby increasing precision in patient management. Consequently, lung function quantification is now considered a cornerstone of the guidelines for asthma diagnosis and management by the Canadian Thoracic Society[64]. Asthma, the most common chronic childhood condition[62], is an obstructive lung disease characterized by airflow limitation due to airway narrowing, which leads to increased resistance.

2.1 Measuring Resistance

2.1.1 Spirometry

Resistance can be measured directly or indirectly. The current gold standard diagnostic test for adults uses spirometry, which evaluates resistance indirectly based on flow or volume measured as a function of time. It involves special breathing maneuvers administered by qualified personnel[65]. The subject is asked to fully inhale to maximum inspiration, take a brief pause, then quickly exhale as forcefully, completely and for as long as possible[65]. Forced vital capacity (FVC) is the volume of air expired by maximal effort after a maximum inhalation. Forced expiratory volume in 1 second (FEV1) is the volume of air expired in the first second of the FVC maneuver. Since mechanical properties of the central airways affect expiratory resistance, both FVC and FEV1 are impacted[65].

Part of the popularity of spirometry may be attributed to its ability to distinguish between normal, obstructive, restrictive or potentially mixed lung conditions based on the FEV1/FVC ratio. Another index is the individual value reported as a percentage of predicted value calculated from well-established population-specific reference equations[65]. An FEV1/FVC of at least 0.70 or the FEV1 and FVC % predicted of at least 80% are considered normal[65]. The lower limit of normal (LLN) has been gaining support as a better index to establish spirometry norms, as it changes with age. In obstructive lung diseases, airflow limitation decreases FEV1, while FVC may be normal or decreased[65]. In restrictive lung diseases, lung volume limitation compromises FVC and FEV1[65]. However, the considerable subject comprehension and cooperation required in spirometry renders it unfeasible for infants.

2.1.2 Rapid Thoracic Compression (RTC)

The unique breathing maneuver of spirometry can, however, be simulated in infants using rapid thoracic compression (RTC) techniques, in which infants wear an inflatable jacket that applies pressure to the trunk, triggering a 'forced exhalation'[9]. In one method, pressure is applied to a spontaneously breathing sedated infant at end-inspiration, when lung volume consists of FRC and V_T[9]. It generates a partial expiratory flow-volume loop from which the presence of airflow obstruction can be identified[9]. Since flow depends on volume, the reference flow used is at end-expiration, when lung volume consists of FRC, while maximum flow at FRC ($V'_{max,FRC}$) is reported. However, pre-term infants tested using this technique had an unstable volume axis, which reduced the reproducibility and generalizability of this procedure[9].

Another RTC method is the raised volume-rapid thoracic compression (RV-RTC) technique, which utilizes the Hering-Breuer reflex, inhibiting spontaneous breathing at high lung volumes[66]. The reflex is prominent in infants and diminishes with age. It is invoked by preceding the forced exhalation with inflations to raise the lung volume of the sedated infant (Fig. 14[66]).

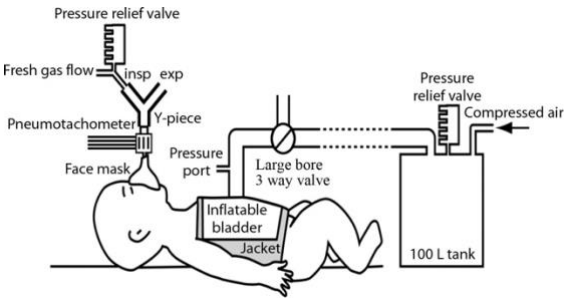

Figure 14. Raised volume-rapid thoracic compression (RV-RTC) technique to simulate forced expiration in infants

The main concern surrounding these techniques is the need for sedation, typically contraindicated in infants. Additionally, all spirometry tests can only be performed by qualified personnel, limiting its accessibility in routine clinical care.

2.1.3 Limitations of Spirometry

Sedation is contraindicated in infants due to their unique breathing pattern and immature respiratory control[22]. In addition to the risk of potential adverse effects of sedation in adults, it has the added risk in infants to weaken or even inactivate the adaptive mechanisms used to maintain a dynamically elevated FRC[22]. These risks are compounded in pre-term and term infants with lung disease or neuromuscular disorders[9,22]. Furthermore, the effects and metabolism of sedation are different in different infants, introducing variability in measurements obtained under sedation that is difficult to control[9,67]. Techniques requiring sedation are also less feasible in studies conducted in community settings, such as the ongoing research in Uganda led by P. Moschovis (unpublished), and healthy infants, like in our study, as there is little benefit for the risks incurred[67].

Forced maneuvers reflect different aspects of lung physiology compared with tidal breathing. Forced expiration places the respiratory system at its mechanical limits to relay specific information that differs from that obtained by oscillometry[9]. Because subjects breathe spontaneously during OSC, it provides structural information from the respiratory system at its regular resting state.

Spirometry is the current de facto standard to evaluate human lung mechanics[17], which may explain the ample clinical evidence available correlating its parameters to pathology. Oscillometry is its counterpart in animal models[68], since spirometry cannot be used meaningfully in animal models[17]. It is rare for the commonly used technique in human assessment to not also be used in animal models studying human disease[17], as it greatly limits vital translational research. Although oscillometry can be applied to both humans and animal models, it is currently limited to human research settings, not routine clinical practice, which may explain the present uncertainty in correlating its parameters to pathology[17]. A database of human OSC data has the potential to provide robust evidence to link OSC indices to specific lung diseases[17] and derive pertinent information of clinically meaningful significance.

In addition to sedation, the need for specialized technicians and subject cooperation, as well as equipment cost, further limit the accessibility of spirometry[9]. As a result, most Canadian asthma patients have not undergone spirometry to support diagnosis, monitor disease progression or adjust treatment[69], contrary to established recommendations[70,71]. On the other hand, oscillometry requires no sedation, specialized personnel or subject cooperation, making it more accessible to routine clinical care. Most importantly, spirometry is not as sensitive as oscillometry at detecting changes in the small airways. Due to the cross-sectional area of the small airways being so large, a significant loss of this area is required before it can be picked up by spirometry, while oscillometry is capable of detecting minute changes in this region.

2.2 Knowledge Gaps

Despite the advantages of oscillometry that has been encouraging its wider acceptance recently, particularly in infants, more research is required to fill in knowledge gaps. Appropriate quality control measures and population-specific reference values are some areas that require further investigation[9].

2.2.1 Quality Control

Coherence (COH) and coefficient of variation (CV) are commonly used to report reproducibility of measurements. In the early days of oscillometry, low COH was considered a criterion to discard measurements, as it was thought to indicate the presence of too many artefacts[25]. COH quantifies the linear relationship between pressure and flow at each oscillation frequency, with a value of one denoting a unique impedance perfectly linking P and V' and a cut-off typically set at 0.9[12,19]. Low coherence is caused by noise from artefacts, specifically non-linearities, poor signal-to-noise ratio or contamination from breathing components or cardiogenic oscillations[25]. Recently, the exclusion of measurements solely based on COH has come into question. It may be used to indicate the quality of values obtained by the same device in the same setting, but due to different algorithms used by device manufacturers to calculate COH, absolute values cannot be compared across devices or used to justify discarding measurements[19,25]. Also, it has been

found that coherence is often decreased in disease, potentially introducing bias when an arbitrary cut-off is used[25,72]. Finally, a high coherence value does not necessarily guarantee the absence of noise or measurement errors. As such, coherence is increasingly being replaced by CV as a measure of reproducibility[19,25].

Coefficient of variation (CV) quantifies reproducibility by comparing the standard deviation of data to their mean to detect potential outliers. The latest guidelines from the European Respiratory Society (ERS)[25] recommended the use of three replicates at the lowest frequency to compute CV of R_{rs}. They reported that a CV of 10% or lower for adults and 15% or lower for children indicates sufficient reproducibility of the data, although they noted the lack of current publications to support these cut-offs[25]. However, they maintained the use of arbitrary threshold values would exclude outliers by forcing the selection of measurements close to each other, fulfilling the purpose of CV. This study will use the recommended threshold to help provide support to the guidelines. CV is typically calculated only for R_{rs} because the negative and zero values of X_{rs} complicate matters. At those points, CV would be negative or approaching infinity, leaving COH as the only quality indicator. However, reproducibility does not convey any information about data accuracy, which can be evaluated based on reference values.

2.2.2 Reference Values

Collection of population-specific reference OSC outcomes are currently in progress. While some values and prediction equations now exist for various groups based on sex, age, height and ethnicity of adults and children[19,28,31,73], infant OSC data remain sparse[9]. The use of different devices with varying specifications, protocols and signal analyses restricts the applicability of reference measurements to the specific population evaluated by the specific device[25]. Hence, the only reference values relevant to this study are those reported by research groups who used the wave-tube[26,49–52] and modified C-100[60,61] mentioned previously. The ERS report emphasized the need for OSC normative values, similar to those established by the Global Lung Function Initiative for spirometry[74]. It would require following a standardized protocol using a specific device in multiple countries[25]. Furthermore, the lack of reference data on healthy infants using the same device and methods may lead to misinterpretation of infant lung function data[75]. If values obtained by the tremoFlo® N-100 agree with those from the wave-tube, it will provide a validated commercial device that can be consistently used in future research that aims to establish reference values.

2.3 Rationale

2.3.1 Device Validation

According to Kendig's Disorders of the Respiratory Tract in Children[27], an ideal lung function test should: a) be quick and easy to perform for infants and operators, b) have standard operating procedures,

guidelines and robust healthy reference data available, c) discriminate between healthy infants and those with lung disease, d) be feasible at any age to allow longitudinal follow-up of individuals with lung disease and e) be cheap and widely available to ensure healthcare equality.

With no need for sedation or specialist testers, oscillometry is much easier and quicker to conduct than spirometry. With no need for subject comprehension or cooperation, OSC is feasible in a wider range of populations, like neonates and infants. In 2020, guidelines and recommendations were published to update those from 2003 by the ERS task force on oscillometry[25]. Of the references used to support the previous guidelines, only two out of six were retained for adults in the update, with five newer papers added and only two out of nine were retained for children, with ten newer papers added for children and one for preschoolers. It reflects the evolution of our knowledge and understanding of OSC that has paralleled the fast pace of technological innovation for the past two decades.

This study aims to answer questions in terms of best practices to establish standard operating procedures, with the goal that future studies will establish normal values. The concurrent N-100 studies by the UAB group aim to investigate its ability to detect the difference between health and disease. Finally, verifying the reliability and agreement of measures from the N-100 with those of the wave-tube will provide a validated commercial device that has the potential to enter the market and become widely available.

Furthermore, the use of dynamic impedance to calibrate both devices will strengthen our study, as the static impedance commonly used to date has been found to be less accurate[25,76]. This study also aims to perform breath-by-breath analysis at a single frequency, an emerging area of OSC research that has the potential to enhance the range of clinical information that can be derived from oscillometry[19]. It is yet another aspect of OSC that is missing normative data and standardization[37].

2.3.2 Research Objectives

The primary objective of this study is to validate the tremoFlo® N-100 Airwave Oscillometry System™ by comparing its measurements of respiratory impedance (Z_{rs}), specifically resistance (R_{rs}) and reactance (X_{rs}), with those of the current gold standard OSC device in infants, the wave-tube oscillometer. In so doing, we will determine best practices for successfully acquiring valid measurements from infants. The secondary objective of this study is to identify physiologically meaningful intra-breath patterns of respiratory mechanics by analyzing Z_{rs} recorded at the mono-frequency signal at 16 Hz. We hypothesize that the tremoFlo® N-100 will provide measurements with a high level of reliability and agreement, indicated by an intraclass correlation coefficient (ICC) of at least 0.7 or more. If there is evidence to support our hypothesis, then it will provide a validated commercial device with the potential to become widely available.

Chapter 3: Methodology

3.1 Study Population

3.1.1 Sample Size

With the minimum acceptable reliability between the mean values measured by each device (k = 2) set *a priori* to an intraclass correlation coefficient (ICC) of 0.7 and an expected reliability of 0.97 (α=0.05), it was determined a sample of 7 participants would have 80% power to indicate good reliability[77,78]. To account for potentially unsuccessful tests, a target of 15 subjects was set.

3.1.2 Selection of Study Subjects

Potential study subjects were recruited from the Maternity Care Unit at the Royal Victoria Hospital of the McGill University Health Centre (MUHC – Glen site) from November 2020 to May 2022. Permission was directly sought from the parents of eligible neonates to be contacted after around five to six weeks. This study was approved by the Pediatrics panel of the MUHC Research Ethics Board.

3.1.3 Inclusion and Exclusion Criteria

Parents were approached at the maternity unit only if their newborns were identified by the charge nurse as healthy, with a normal birthweight for gestational age and no neonatal distress or respiratory issues after a term pregnancy of more than 37 weeks. Those with Coronavirus Disease (COVID)-19 symptoms were recruited later over the phone.

After five to six weeks, contact was re-established and the infants underwent further screening to ensure they did not have any acute respiratory illness in the prior month or a diagnosis of any chronic condition that may affect breathing, such as gastroesophageal reflux disease, cystic fibrosis or neuromuscular disease. It was also verified that they were not on any medication, other than vitamins.

3.2 Study Design

For this cross-sectional device validation study, recruitment occurred after delivery at the maternity ward. The informed consent was attached to the email (Appendix B) as a full description of the study to aid parents in the decision-making process with respect to voluntary participation. Consent forms were reviewed and signed in person at the study visit, with a copy for each subject to keep.

3.2.1 Study Location

The Centre for Innovative Medicine (CIM-Pediatrics), a dedicated space for clinical research in the Montreal Children's Hospital at MUHC, was the location chosen to conduct the infant lung function tests. The test room was large enough to accommodate all the study apparatus, two testers, a device operator and a licensed physician, as well as both parents and a stroller or car seat. The room also had all the gear required

to change the baby, like towels and a sink, and resuscitation equipment. It had curtains for privacy while the infant was nursed.

When not in use, the study devices, consumables and laptop were kept in the CIM's storage room, with confidential paperwork in a secure drawer at the office of the study's principal investigator.

3.2.2 Calibration

Current commercial oscillometers usually use a low, static reference impedance for calibration and a rudimentary approach to correct for the impedance of the filter and facemask[76]. However, it was found that systematic errors in Z_{rs} measurements remained in the system, especially at the high impedance values of infants[76]. For this study, both types of calibration, static and dynamic, were performed by the manufacturers of each device using a three-point lung model simulating Z_{rs} changes during tidal breathing to improve accuracy[76].

According to N. Restrepo, MEng, Research & Development Associate at THORASYS (email communication, February 2022), the factory calibration of the tremoFlo® N-100 consists of the static calibration, referred to as channel calibration, and dynamic calibration, referred to as multi-test load calibration. As with any sensor, the pressure and flow sensors of the tremoFlo® are subject to gain and zero offset errors. These errors were accounted for by directly measuring a set of known pressures and flows that were then fitted to each sensor's gain using a stable flow bench system. It set the minimum and maximum values that can be reliably measured by the device.

In the multi-test load calibration, a three-point model was used to derive a QRS value representing any errors remaining in the system. Dynamic calibration consisted of three arrangements, with the first two including test loads of known impedance: a) 25 cm H_2O/L/s test load and three-point model, b) 90 cm H_2O/L/s test load and three-point model and c) zero load calibration with no test load or model attached to the device. The specific antimicrobial filter chosen for the study was part of all three setups to account for its impedance as part of the overall device impedance. The multi-test load calibration sets a limit on the range of impedance values that can be accurately measured with the device. Since the modified C-100® was originally developed for adults, it used test loads measuring 2 and 15 cm H_2O/L/s, which could not compensate for errors potentially present at the high impedance of infants, ultimately reducing accuracy.

Before each test, the device operator ensured the absence of any changes or damage to the system by verifying the validity of the above factory calibration. This end-user verification step used only the higher 90 cm H_2O/L/s test load, as recommended[25], to evaluate how accurately the QRS model of the system can predict known values. The accepted tolerance of the verification was $\leq \pm$ 7% for the tremoFlo® and 5% for the wave-tube, both more conservative than the current recommendation of ± 10%[25].

Since flow and volume are so small in infants, it is very important to minimize the dead space and additional resistance to breathing of the OSC device (recommended: < 1 hPa/L/s or < 1.02 cm H_2O at $\leq$ 5

Hz) and antimicrobial filter (recommended: < 1 hPa/L/s or < 1.02 cm H_2O at ≤ 5 Hz)[25]. Keeping the total equipment dead space and resistance low (recommended: < 2 hPa/L/s or < 2.04 cm H_2O) reduces the possibility of interfering with the breathing pattern, which can increase V_T, depending on the duration of the measurements[25]. As such, the antimicrobial filter available with the lowest resistance was chosen for this study (Medtronic DAR™ Electrostatic Filter Size Small, Mansfield, USA). According to the manufacturer, resistance to airflow of this filter measures 0.7, 2.1 and 3.6 cm H_2O at V_T of 30, 60 and 90 mL, respectively, slightly higher than the guidelines[25]. A bias flow of 2 L/min of medical-grade air connected to the filter by the narrowest tubing available prevented CO_2 rebreathing and continuously flushed equipment dead space.

Details on wave-tube calibration have been reported previously[49]. While the wave-tube accounts for the facemask impedance (BOMImed Air-Flex™ Size 1 Infant, Winnipeg, Canada), the tremoFlo® N-100 does not, treating it instead as a static part of the respiratory system. To explore the impact of the differing approach to facemask impedance, 16-second spectral measurements were made with each device attached to the filter-mask assembly (FMA) on the three-point model originally used to develop the N-100. The FMA was exchanged with a stopper and the same measurements were repeated.

3.2.3 Testing with Each Device

The date of birth, sex and ethnicity were entered into the software of both devices, as the infant was fed and put to sleep by the parents. Since infants in natural rapid eye movement (REM) sleep have a higher breathing frequency and unstable FRC, measurements were taken during deep, non-REM sleep, confirmed by visual inspection of the infant[22,79]. Once achieved, the infant was placed supine on the bed, with the neck slightly extended via a shoulder roll and head supported by a parent to face forward. Measurements in the supine position were found to be reproducible[80] and avoided forward slouching, which could compress the abdomen and move its contents upwards into the thorax, leading to some airway narrowing and decreased lung volume. Extending the neck prevents downward head tilts, which could compress the throat and increase upper airway resistance. Head stabilization by the parent also avoided the potentially compounding effects of head rotations on impedance[81].

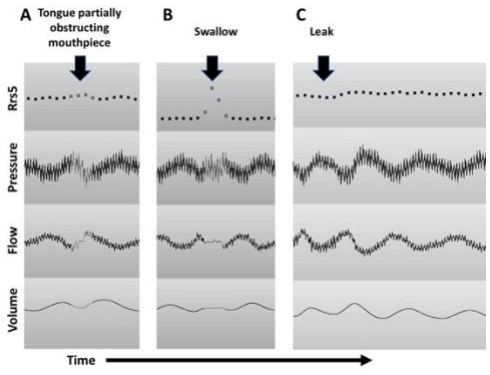

Figure 15. Recording display of tongue obstruction, swallows and facemask leaks

The first device used to measure impedance was randomized by alternating between the tremoFlo® and the wave-tube for each infant. The facemask was gently but firmly placed on the face to form a tight seal around the nose and mouth. With the most common source of error in infant testing being leaks around the mask, its position was checked before and throughout the test. The tester stationed at the laptop

visually identified leaks (Fig. 15[25]) during recording, as indicated by sudden large decreases in the absolute magnitude of Z_{rs}, with subtle changes in the flow and volume signals.

While the infant breathed quietly through the mask, vibrations ranging from 7 to 41 Hz and 8 to 48 Hz were applied by the tremoFlo® and the wave-tube, respectively. Then, the 16 Hz measurement was recorded for intra-breath analysis. Attempts were made to obtain at least three measurements for up to 60 seconds, or as long as tolerated by the infant, with the goal of collecting at least three technically acceptable 10 to 30-second data epochs from the tests.

Proper training from device manufacturers and knowledge of respiratory physiology allowed adequate real-time quality control and physiologically meaningful data interpretation. Pauses in the volume signal with zero flow or sudden changes or spikes in resistance and pressure represented swallows, breath holds, vocal cord closures and facemask leaks (Fig. 15[25]). Large impedance values at zero flow were considered transient airway occlusions or swallows, while negative R_{rs} values were known to be physiologically impossible[25]. Notes on infant behavior causing noise artefacts such as cries, coughs, snores and sighs, were made to help correctly interpret the lung function data[22].

The infant's weight and height were measured using a digital neonatal scale with a built-in measuring tape (Rice Lake Weighing Systems Healthweigh®, Rice Lake, USA), either before or after testing, based on parental preference. A questionnaire, included in Appendix A (Fig. A1), was completed by the parents after the test to collect feedback on the tolerability and acceptability of the test. A technician questionnaire (Fig. A2) was also completed by the device operator to record ease of device set-up, calibration and use.

3.3 Statistics

This validation study used both coherence (COH) and coefficient of variation (CV) to report reproducibility, or the extent to which repeated measurements are similar. Reproducibility, or repeatability, drops when there are issues in accuracy, precision or both. To be included in data analysis, R_{rs} at 7 Hz needed a COH greater than 0.5 and a CV of 15% or lower.

Agreement involves accuracy, as it assesses the closeness of repeated measurements taken from the same subject (intrasubject variability) by estimating measurement error[82]. Reliability involves precision, as it assesses whether subjects can be distinguished from one another (intersubject variability), despite measurement errors[82]. Reliability depends on the heterogeneity of the study sample, while agreement is a characteristic of the measurement instrument itself. As such, reliability is key for instruments used for distinction, like distinguishing healthy subjects from those with disease. On the other hand, agreement is key for instruments used for evaluation, like changes in lung resistance over time[82].

3.3.1 Intraclass Correlation Coefficient (ICC)

To assess the reliability of repeated measurements on a continuous scale, intraclass correlation coefficient is considered the most appropriate[82]. ICC links measurement error to intersubject variability using: $ICC = \frac{intersubject\ variability}{intersubject\ variability + measurement\ error}$[82]. When measurement error is small relative to intersubject variability, ICC approaches 1, indicating high reliability, as measurement error has minimal effect on the ability of the device to distinguish subjects. When measurement error is large relative to intersubject variability, ICC approaches 0, indicating low reliability, as measurement error has a large impact on the ability of the device to distinguish subjects.

Two types of ICC can be calculated, one that accounts for systematic differences ($ICC_{agreement}$) and one that does not ($ICC_{consistency}$)[82]. It should be emphasized that ICC is a measure of reliability, despite the term 'agreement' used in its classification[82]. This study included systematic differences between devices by using the formula:

$$ICC = \frac{\sigma^2_{subject}}{\sigma^2_{subject} + \sigma^2_{device} + \sigma^2_{residual}} \quad (16)$$

Subject variance ($\sigma^2_{subject}$) represents variability between subjects, device variance (σ^2_{device}) represents variability due to systematic differences between devices and residual variance ($\sigma^2_{residual}$) represents interaction between subjects and devices. The measurement error, or error variance (σ^2_{error}), is made up of σ^2_{device} and $\sigma^2_{residual}$[82]. The measurement error is represented by the standard error of measurement (SEM), which is the square root of the error variance[82]:

$$SEM = \sqrt{\sigma^2_{error}} = \sqrt{(\sigma^2_{device} + \sigma^2_{residual})} \quad (17)$$

3.3.2 Bland-Altman 95% Limits of Agreement (LoA)

Agreement estimates measurement error in repeated measurements from the same subject. The Bland-Altman 95% Limits of Agreement was used to measure agreement between values derived by the tremoFlo® N-100 and wave-tube. Measurements from one device consistently exceeding the other is an indicator of bias, which is estimated by the mean difference[83]. Variation around the mean is estimated by the standard deviation of the differences. These estimates only apply given that bias and variability are uniform throughout the range of measurements, which can be verified using graphs.

The simplest way to graph the data is to plot the values from each device on each axis[83]. Using the same scale for each axis would produce a line of equality at 45°. If values from both devices are in perfect agreement, then all the datapoints would lie on this line. However, this plot may obscure relevant information should the measurements contain large variation relative to the differences between measurements made by each device.

The recommended method to graph the data is to plot the differences between measurements made by each device on the y-axis and the average of measurements made by both devices on the x-axis for each subject[83]. Any extreme outliers are shown more clearly and any relationship between absolute differences and averages can be investigated further. Plotting the difference in measurements against the measurement from only one device, instead of the average of both devices, is not recommended, even if it is the gold standard device[83]. The average of measurements made by both devices is used as the best estimate of the 'true' value. Using the same scale for each axis helps show the discrepancies relative to the size of the measurements. However, this is impractical when there is very close agreement and may once again obscure important information.

One solution is to add the 95% limits of agreement to the graph. It is estimated by the mean difference ± 1.96 times the standard deviation of the differences[83]. If there is close agreement, then 95% of the datapoints should lie within this interval, assuming that the mean difference and the standard deviation of the differences are normally distributed.

Chapter 4: Results

The first part of the study consisted of internal validation of the tremoFlo® N-100, as different methods were attempted to determine the optimal technique of acquiring measurements from infants with the device. Sleep state (awake but calm vs. asleep), sleep position (bed vs. parent's arms vs. car seat or stroller), neck position (extension via shoulder roll vs. parent's arm) and bias flow (with vs. without) were compared.

The second half of the study consisted of external validation by comparing measurements made by the tremoFlo® N-100 with those from the Wave-tube Oscillometer. The protocol was modified to obtain a few, longer recordings, lasting a maximum of 120 seconds, as they proved more practical and feasible than the shorter, multiple measurements made in the first part[25]. The rim of the facemask was inflated and remained in place, instead of being removed between each measurement.

4.1 Demographics

The demographics, anthropometrics and testing conditions of the infants from the first part of the study (n = 14, 9 females, 5 males) are listed in Table 2. The mean ± SD age, weight and height were 10.47 ± 1.59 weeks, 5.37 ± 0.77 kg and 58.4 ± 3.1 cm, respectively. Most infants were fed at the visit, tested supine on the bed with the neck extended via a shoulder roll and were not swaddled. Values of the last 3 infants in the table were excluded from analysis, as the tubing detached from the adaptor connecting it to the base unit, invalidating the data due to potential leaks in the equipment.

Table 2. Characteristics of the study population from the internal validation (WT = weight, HT = height, F = female, M = male, Y = yes, N = no)

	ID	Age (wks)	WT (kg)	HT (cm)	Sex	Fed	Sleep state	Neck position	Sleep position	Bias Flow	Wraps used
1	4	11.14	5.00	60.0	F	Y	awake, content	extended via shoulder roll	bed	no	no
2	12	11.29	5.40	55.0	F	Y	awake, content	extended via shoulder roll	bed	no	swaddled
3	2	13.57	6.10	60.0	M	Y	awake, content	extended via shoulder roll	bed	no	no
4	16	10.14	5.30	56.5	F	Y	awake, not quite content	extended via shoulder roll	bed	no	no
5	21	9.14	5.50	56.0	F	N	awake, not quite content	extended via shoulder roll	bed	no	no
6	18	10.14	7.10	64.0	M	Y	awake, not quite content	extended via shoulder roll	arms	no	no
7	19	10.29	5.69	59.5	M	N	asleep	relaxed	arms	no	no
8	15	11.71	5.30	59.0	F	Y	asleep	extended via parent's arm	bed	no	no
9	25	11.43	5.50	59.0	F	Y	asleep	extended via shoulder roll	bed	yes	no
10	26	11.86	4.30	55.0	F	Y	asleep	relaxed	arms	yes	no
11	36	7.29	4.80	53.5	F	Y	asleep	extended via shoulder roll	bed	yes	swaddled

12	33	8.14	4.90	60.0	M	Y	awake, content	no shoulder roll	car seat	yes	no
13	35	10.14	6.20	63.0	M	Y	asleep	extended via shoulder roll	bed	yes	swaddled
14	32	10.29	4.10	56.5	F	Y	asleep	extended via shoulder roll	bed	yes	blanket

The demographics, anthropometrics and testing conditions of the infants from the second part of the study (n = 13, 7 females, 6 males) are listed in Table 3. The mean ± SD age, weight and height were 10.16 ± 1.52 weeks, 5.18 ± 0.62 kg and 57.7 ± 2.0 cm, respectively.

Of the 13 infants, 3 did not fall asleep (ID 47, 48 and 73), 2 were tested with only the tremoFlo® N-100 (ID 85 and 95) and 2 were tested in the stroller (ID 57 and 64).

Table 3. Characteristics of the study population from the external validation (WT = weight, HT = height, F = female, M = male, Y = yes, N = no)

	ID	**Age (wks)**	**WT (kg)**	**HT (cm)**	**Sex**	**Fed**	**Sleep state**	**Neck position**	**Sleep position**	**Bias Flow**	**Wraps used**
1	47	10.57	N/A	N/A	M	Y	awake not tested	extended via shoulder roll	bed	yes	no
2	48	10.43	N/A	N/A	M	N	awake not tested	extended via shoulder roll	bed	yes	no
3	57	10.00	5.40	55.0	F	Y	asleep	no shoulder roll	stroller	yes	blanket
4	56	11.43	5.90	58.0	F	Y	asleep	extended via shoulder roll	bed	yes	no
5	**58**	11.57	5.70	57.0	F	Y	asleep	extended via shoulder roll	bed	yes	blanket
6	61	10.86	5.40	60.0	M	Y	asleep	shoulder roll on bed but positioned lower down thus no neck extension	bed	yes	swaddled
7	64	10.14	4.50	60.2	M	Y	asleep	extended via shoulder roll	stroller	yes	blanket
8	**84**	7.14	4.93	59.0	M	Y	asleep	extended via mother's arm	arms	yes	no
9	85	7.29	4.45	56.0	F	Y	asleep	extended via shoulder roll	bed	yes	no
10	73	10.71	N/A	N/A	F	Y	awake not tested	extended via shoulder roll	bed	yes	no
11	**86**	10.14	5.90	59.0	M	Y	asleep	extended via shoulder roll	bed	yes	blanket
12	**94**	8.86	4.40	55.5	F	Y	asleep	extended via shoulder roll	bed	yes	no
13	95	8.71	N/A	N/A	F	Y	asleep	extended via shoulder roll	baby carrier on bed	yes	blanket

4.2 Data Analysis

Values of the 11 participants included in the analysis for internal validation are shown in Table 4. Only impedance at 16 Hz was recorded for the first 3 subjects, while it was not obtained in subject ID 16, 21, 18 and 26. All subjects were within the reproducibility threshold, except ID 19 with a CV of 40.95%. All infants with spectral values reached f_{res}, except ID 36. Summary statistics are in Table 5.

COH was higher in asleep infants (Table 3 ID 19, 15, 25, 26 and 36), compared with those awake (Table 3 ID 16, 21 and 18; mean ± SD COH 0.94 ± 0.03 vs. 0.70 ± 0.08, respectively). CV improved with the use of bias flow (Table 3 ID 25, 26 and 36), compared with infants tested without bias flow in either sleep state (Table 3 ID 16, 21, 18, 19 and 15; mean CV 2.50 vs. 14.57, respectively). There was no correlation between impedance and weight, height or sex.

Table 4. Mean OSC and reproducibility values of all participants included in the internal validation (R_{rs}, X_{rs} in cm $H_2O/L/s$; AX in cm H_2O/L; f_{res} in Hz)

	ID	R16	X16	R7	X7	R19	X19	R7-19	AX	fres	CV7 (%)	COH7
1	4	25.58	-12.58	N/A	N/A	N/A	N/A	N/A	N/A	N/A	N/A	N/A
2	12	35.23	-16.37	N/A	N/A	N/A	N/A	N/A	N/A	N/A	N/A	N/A
3	2	31.99	-18.39	N/A	N/A	N/A	N/A	N/A	N/A	N/A	N/A	N/A
4	16	N/A	N/A	45.73	-20.09	38.43	-7.80	7.30	211.06	26.14	10.38	0.79
5	21	N/A	N/A	40.71	-17.82	31.88	-15.30	8.83	364.17	34.18	7.46	0.68
6	18	N/A	N/A	42.17	-22.72	30.88	-12.03	11.29	367.55	37.41	4.63	0.63
7	19	39.61	-22.71	12.38	-2.57	11.87	-0.97	0.51	27.97	16.40	40.95	0.91
8	15	5.79	0.94	8.61	-0.30	8.39	0.78	0.22	0.55	10.28	9.42	0.99
9	25	17.72	-3.75	24.47	-8.48	18.67	-4.68	5.80	123.86	38.26	1.85	0.94
10	26	N/A	N/A	20.74	-4.61	19.17	-4.17	1.57	94.89	39.17	1.63	0.94
11	36	34.55	-15.16	39.37	-24.70	30.84	-9.11	8.53	340.91	N/A	4.01	0.91

Table 5. Mean ± SD of OSC variables from participants included in the internal validation (R_{rs}, X_{rs} in cm $H_2O/L/s$; AX in cm H_2O/L; f_{res} in Hz)

OSC Variables	Mean	SD	OSC Variables	Mean	SD
R7	29.27	14.53	**X7**	-12.66	9.74
R19	23.77	10.73	**X19**	-6.66	5.46
R7-19	5.51	4.23			
f_{res}	28.84	11.57	**AX**	191.37	151.48
R16	27.21	11.88	**X16**	-12.57	8.35

Measurements from the wave-tube and tremoFlo® are shown in Table 6. Valid spectral impedance from both devices were obtained from 4 infants (ID 58, 84, 86 and 94). All subjects were within the reproducibility threshold using the wave-tube. However, IDs 84 and 86 had a CV of 18.7% and a COH of 0.41, respectively, with the tremoFlo®. All infants reached f_{res}, except ID 86 with both devices and 84 with tremoFlo® only. Summary statistics are in Table 7, while descriptive statistics are in Appendix C (Table C1).

Table 6. Mean OSC and reproducibility data of all participants included in the external validation of the tremoFlo® with the wave-tube (R_{rs}, X_{rs} in cm H_2O/L/s; AX in cm H_2O/L; f_{res} in Hz)

R7	**wave-tube**	**tremoFlo**	**X7**	**wave-tube**	**tremoFlo**
58	54.0	38.0	**58**	-10.9	-17.6
84	45.7	35.0	**84**	-19.0	-22.7
86	59.9	31.0	**86**	-36.5	-19.6
94	44.5	38.0	**94**	-15.2	-20.6
R13	**wave-tube**	**tremoFlo**	**X13**	**wave-tube**	**tremoFlo**
58	45.3	30.5	**58**	-9.5	-13.8
84	39.1	28.0	**84**	-11.5	-12.7
86	73.2	27.8	**86**	-26.0	-11.9
94	39.4	28.5	**94**	-5.3	-11.2
R19	**wave-tube**	**tremoFlo**	**X19**	**wave-tube**	**tremoFlo**
58	41.8	26.2	**58**	0.26	-5.21
84	35.8	28.0	**84**	-7.29	-7.76
86	61.4	23.5	**86**	-22.88	-9.47
94	38.1	28.4	**94**	-0.55	-6.16
R29	**wave-tube**	**tremoFlo**	**X29**	**wave-tube**	**tremoFlo**
58	45.0	27.6	**58**	6.70	0.66
84	35.2	26.9	**84**	-1.67	-3.26
86	53.0	20.8	**86**	-13.93	-4.88
94	36.6	26.1	**94**	6.12	-5.31
R37	**wave-tube**	**tremoFlo**	**X37**	**wave-tube**	**tremoFlo**
58	41.8	28.0	**58**	7.18	2.09
84	34.2	27.2	**84**	1.99	-1.37
86	49.0	21.0	**86**	-11.61	-3.59
94	37.3	25.8	**94**	11.29	3.98
R7-19	**wave-tube**	**tremoFlo**	**R7-29**	**wave-tube**	**tremoFlo**

58	12.2	11.8	**58**	9.0	10.4
84	9.9	7.1	**84**	10.5	8.1
86	-1.5	7.5	**86**	6.8	10.2
94	6.4	9.5	**94**	7.9	11.9
fres	**wave-tube**	**tremoFlo**	**AX**	**wave-tube**	**tremoFlo**
58	18.6	27.6	**58**	89.0	174.1
84	29.0	0.0	**84**	195.9	246.5
86	0.0	0.0	**86**	679.6	275.3
94	17.8	34.2	**94**	79.7	218.5
COH7	**wave-tube**	**tremoFlo**	**CV7**	**wave-tube**	**tremoFlo**
58	0.987	0.973	**58**	9.4%	13.0%
84	0.977	0.943	**84**	10.6%	18.7%
86	0.998	0.405	**86**	0.5%	10.5%
94	0.974	0.983	**94**	11.5%	14.3%
R16	**wave-tube**	**tremoFlo**	**X16**	**wave-tube**	**tremoFlo**
56	46.5	27.0	**56**	-17.7	-8.3
58	47.0	26.7	**58**	-9.2	-9.6
61	32.6	24.2	**61**	-6.6	-11.1

Table 7. Mean ± SD of differences between wave-tube and tremoFlo® measurements of OSC variables (R_{rs}, X_{rs} in cm $H_2O/L/s$; AX in cm H_2O/L; f_{res} in Hz)

OSC Variables	Mean Difference	SD Difference	OSC Variables	Mean Difference	SD Difference
R7	15.5	9.7	**X7**	-0.3	11.2
R13	20.6	16.7	**X13**	-0.6	9.2
R19	17.7	13.8	**X19**	-0.47	8.96
R29	17.1	10.8	**X29**	2.50	8.69
R37	15.1	9.1	**X37**	1.94	6.83
R7-19	-2.2	5.1	**R7-29**	-1.6	2.9
f_{res}	0.9	19.9	**AX**	32.5	250.5
COH7	0.158	0.291	**CV7**	-6.12%	3.52%
R16	16.1	6.6	**X16**	-1.5	7.1

4.2.1 Validity

Intraclass correlation coefficient (ICC) was calculated using the open-source software RStudio (R Foundation for Statistical Computing, Vienna, Austria} using a two-way model that accounted for systematic differences between the average of repeated measures to assess the reliability of measurements

(Table 8). X37 showed excellent reliability (ICC $\geq$ 0.75), while X19, X29, R7-19 and AX were modestly (0.39 < ICC < 0.75) reliable. High reliability indicates that measurement error of these variables was small relative to intersubject variability. The poor reliability of most variables is expected due to the small number of subjects with comparable data from both devices. Thus, results should be interpreted with caution.

Table 8. Reliability of OSC variables measured by ICC

OSC Variables	ICC	OSC Variables	ICC
R7	-0.245	**X7**	0.107
R13	-0.0404	**X13**	-0.0494
R19	-0.278	**X19**	0.559
R29	-0.255	**X29**	0.435
R37	-0.274	**X37**	0.769
R7-19	0.54	**R7-29**	-3.35
f_{res}	0.333	**AX**	0.451
R16	0.148	**X16**	-5.96

Resistance and reactance at frequencies of 7, 13, 19, 29 and 37 Hz, frequency dependence of R_{rs} (R7-19 and R7-29), resonant frequency (f_{res}) and reactance area below f_{res} (AX) were analyzed using Bland-Altman 95% Limits of Agreement. Agreement estimates measurement error in values derived by the wave-tube and tremoFlo® N-100 from the same infant. The difference between measurements were plotted on the y-axis and the average of measurements were plotted on the x-axis for each subject (Table 9). The upper and lower 95% limits of agreement (dashed lines), estimated by the mean difference (dotted lines) ± 1.96 times the standard deviation of the differences[83], are labelled on the secondary y-axis.

Although the plots reveal an outlier, every datapoint lies within the 95% limits of agreement interval, indicating close agreement. However, normal distribution of the mean difference and SD of differences cannot be determined due to the small sample size.

Resistance measured by the tremoFlo® is consistently lower than that measured by the wave-tube by a margin of 15-20 cm H_2O/L/s at all frequencies, indicating bias. The mean differences in reactance and f_{res} are very close to zero, indicating small measurement errors and close agreement. Mean difference of R7-29 is closer to zero than R7-19. AX shows the largest measurement error.

Table 9. Bland-Altman plots of absolute differences in OSC parameters measured by the wave-tube and tremoFlo® N-100 for each infant (dashed lines = 95% limits of agreement; dotted lines = mean difference; grey shading = 95% confidence intervals)

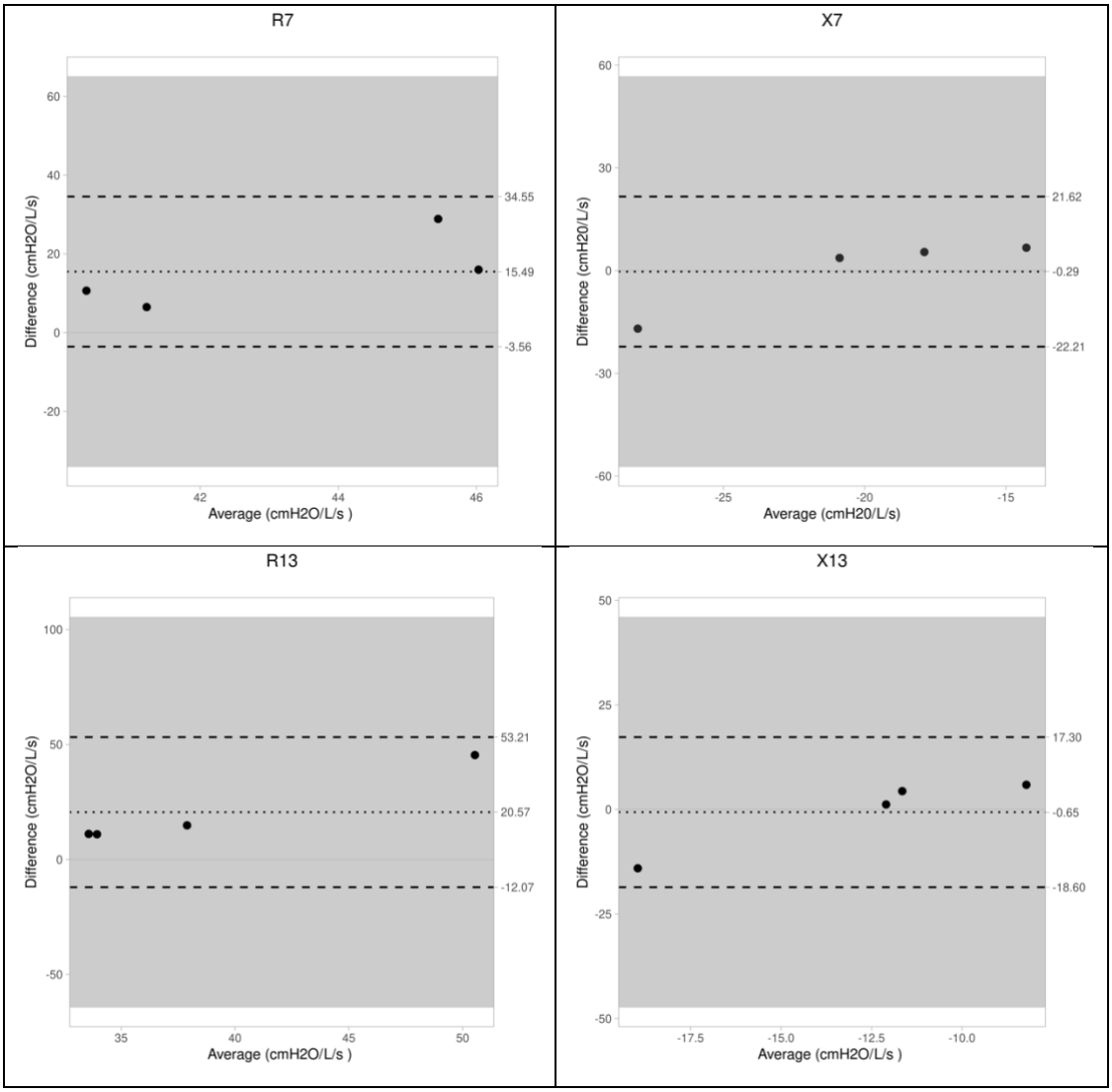

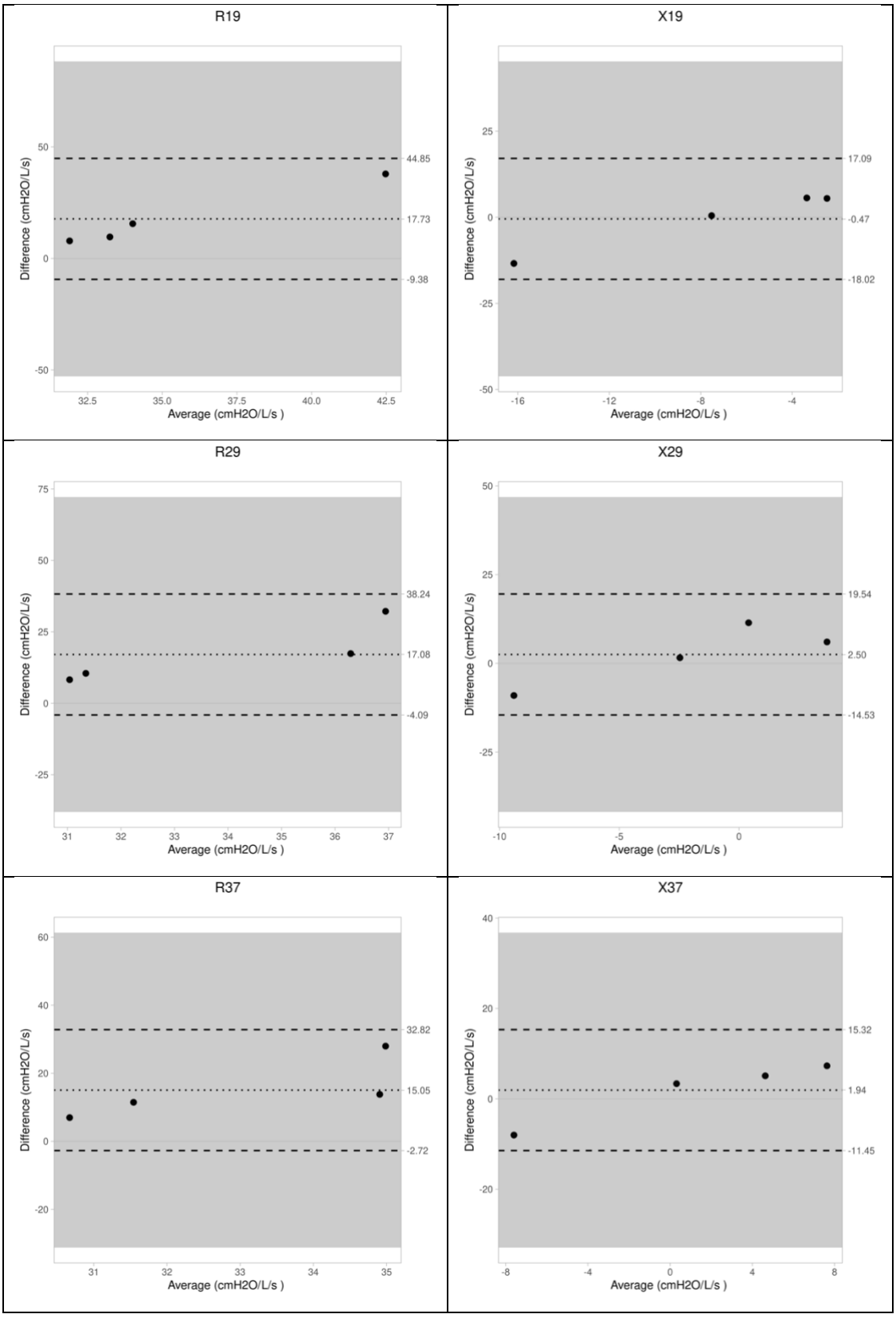
R19
Difference (cmH2O/L/s)
50
0
-50
44.85
17.73
-9.38
32.5
35.0
37.5
40.0
42.5
Average (cmH2O/L/s)
X19
Difference (cmH2O/L/s)
25
0
-25
-50
17.09
-0.47
-18.02
-16
-12
-8
-4
Average (cmH2O/L/s)
R29
Difference (cmH2O/L/s)
75
50
25
0
-25
38.24
17.08
-4.09
31
32
33
34
35
36
37
Average (cmH2O/L/s)
X29
Difference (cmH2O/L/s)
50
25
0
-25
19.54
2.50
-14.53
-10
-5
0
Average (cmH2O/L/s)
R37
Difference (cmH2O/L/s)
60
40
20
0
-20
32.82
15.05
-2.72
31
32
33
34
35
Average (cmH2O/L/s)
X37
Difference (cmH2O/L/s)
40
20
0
-20
15.32
1.94
-11.45
-8
-4
0
4
8
Average (cmH2O/L/s)

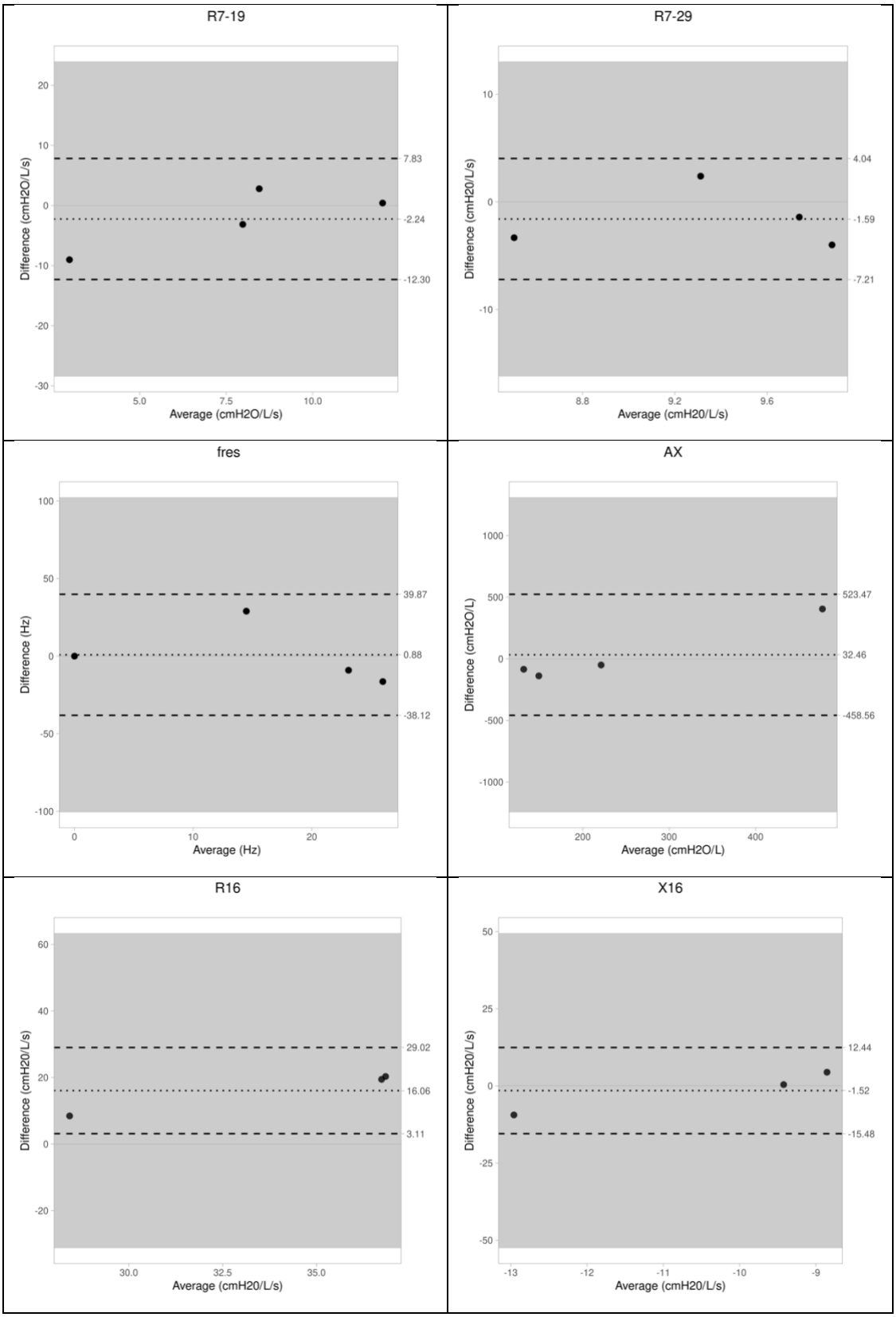
R7-19
Difference (cmH2O/L/s)
Average (cmH2O/L/s)
7.83
-2.24
-12.30
R7-29
Difference (cmH20/L/s)
Average (cmH20/L/s)
4.04
-1.59
-7.21
fres
Difference (Hz)
Average (Hz)
39.87
0.88
-38.12
AX
Difference (cmH2O/L)
Average (cmH2O/L)
523.47
32.46
-458.56
R16
Difference (cmH20/L/s)
Average (cmH20/L/s)
29.02
16.06
3.11
X16
Difference (cmH20/L/s)
Average (cmH20/L/s)
12.44
-1.52
-15.48

4.2.2 Intra-Breath Tracking

Valid 16 Hz measurements from both devices were obtained in one infant (ID 58) and from wave-tube only in two infants (ID 56 and 61). ID 56 woke up before tremoFlo® at 16 Hz, the last recording, could be performed, while the valid segment for ID 61 was only six seconds long using the tremoFlo®, which cannot be reliably compared to the wave-tube.

Intra-breath analysis was possible for ID 58, as there were 4 steady-state segments of 10-15s from both devices. Figure 16 shows graphs of the first segment from the wave-tube, with the time graphs showing the infant's steady breathing pattern throughout the segment (Fig. 16a), while Z vs. V and V' graphs are normalized to a scale of -40 to 100 cm H_2O/L/s (Fig. 16b). Z is split into R and X vs. V and V' in the final set (Fig. 16c).

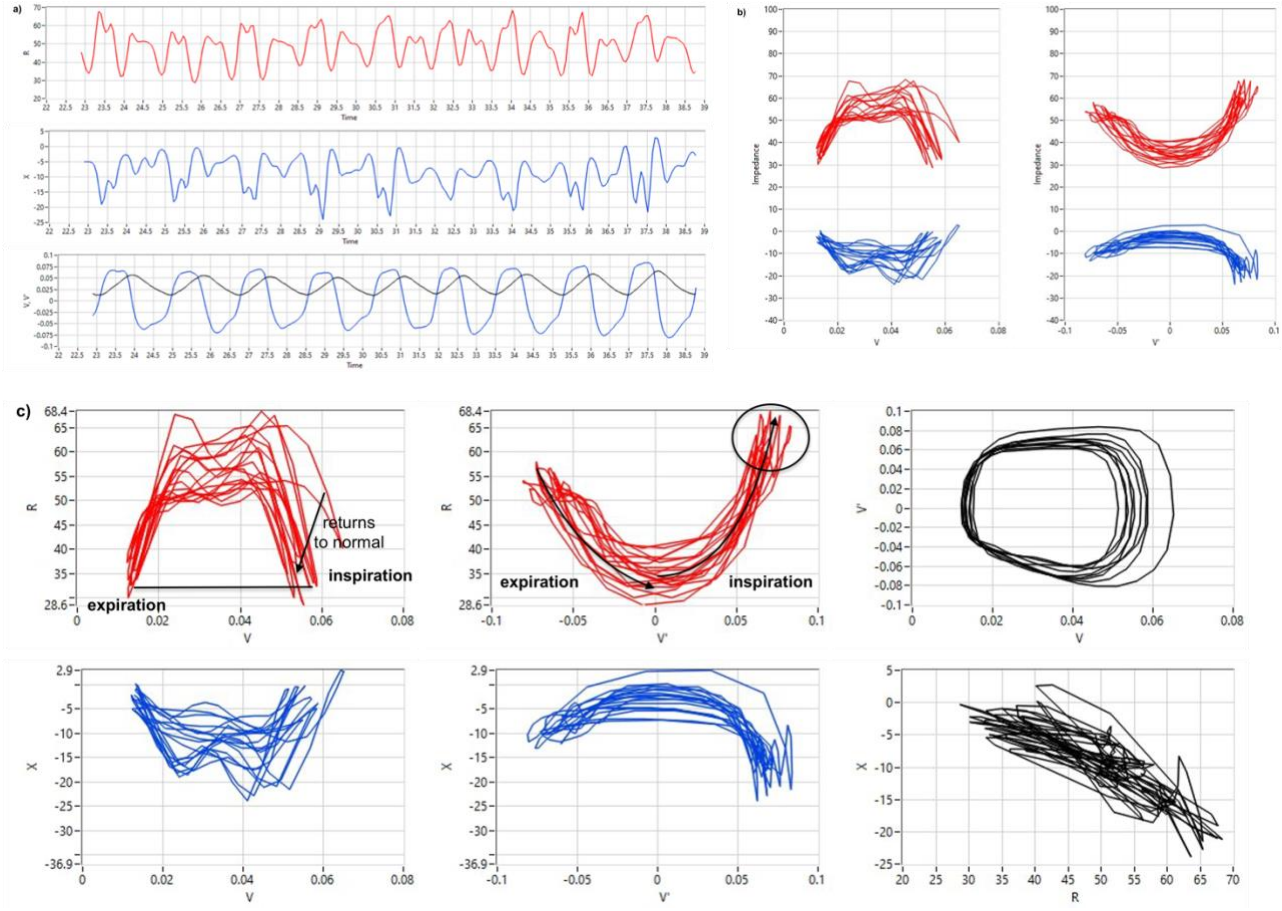

Figure 16. Intra-breath tracking graphs of the first wave-tube segment for ID 58: a) R, X, V and V' vs. time graphs showing steady state, b) normalized Z vs. V and V' and c) R and X vs. V and V', V'-V and X-R graphs

The first wave-tube segment (Fig. 16c) shows high flow dependence because R rises more during inspiration (circled in R-V' curve), which can be attributed to the higher resistance imparted by the nasal pathway when the nares retract during inhalation, akin to a sniff maneuver. Resistance eventually returns to normal, indicated by the arrow in the R-V curve, ultimately with R at end-inspiration and end-expiration

relatively equal, shown by the straight line in the R-V curve. Consequently, the R-V' curve exhibits a non-linear flow dependence.

For the remaining segments, only the final set of graphs are included, as they convey intra-breath information the most clearly.

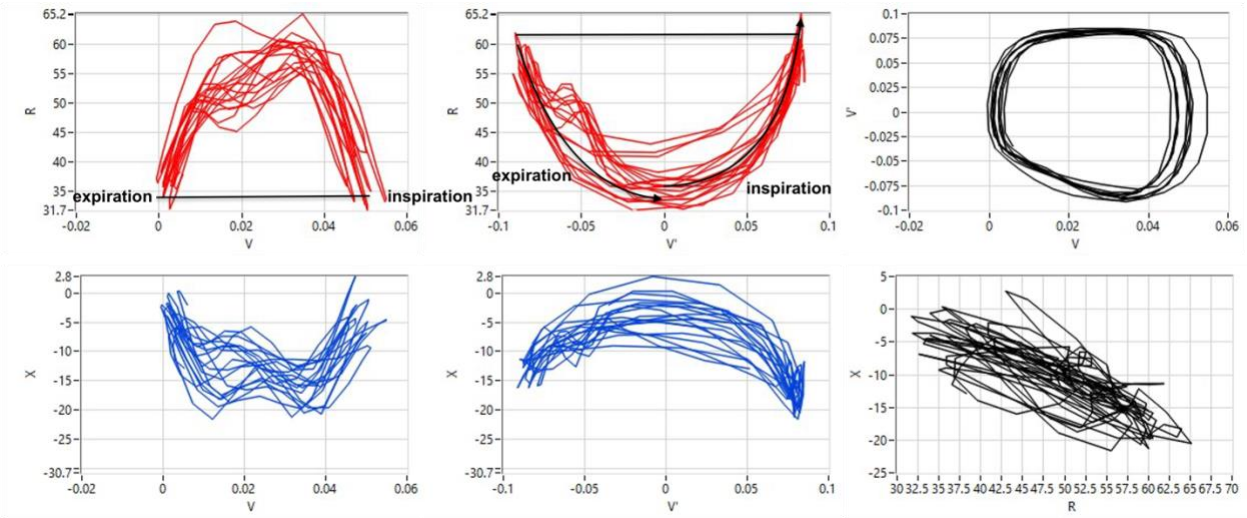

Figure 17. R-V, R-V', X-V, X-V', V'-V and X-R graphs of the second wave-tube segment for ID 58

In the second wave-tube segment (Fig. 17), there is less of a difference in R between inspiration and expiration, which starts from around 30 to 35 cm H_2O/L/s (line in R-V curve) and peaks at around 60 cm H_2O/L/s (line in R-V' curve). This doubling of resistance is consistent in all wave-tube segments.

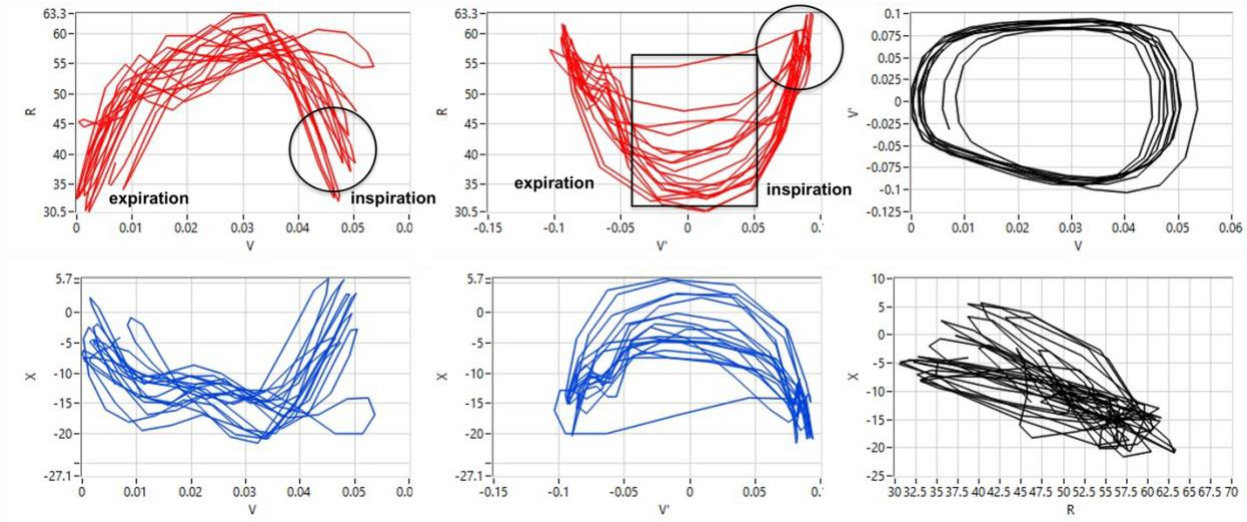

Figure 18. R-V, R-V', X-V, X-V', V'-V and X-R graphs of the third wave-tube segment for ID 58

The third wave-tube segment (Fig. 18) depicts higher end-inspiratory R (circled in R-V curve). The irregular R-V' curve signifies airway closure almost occurring at peak inspiration (circled in R-V' curve),

but then it resolves very gradually (rectangle in R-V' curve). This is a normal phenomenon that often occurs in infants. The lower C_L relative to C_{CW}, causes the closing volume to be greater than FRC in infants, such that the small airways are at risk of collapse during normal tidal breathing[4,9].

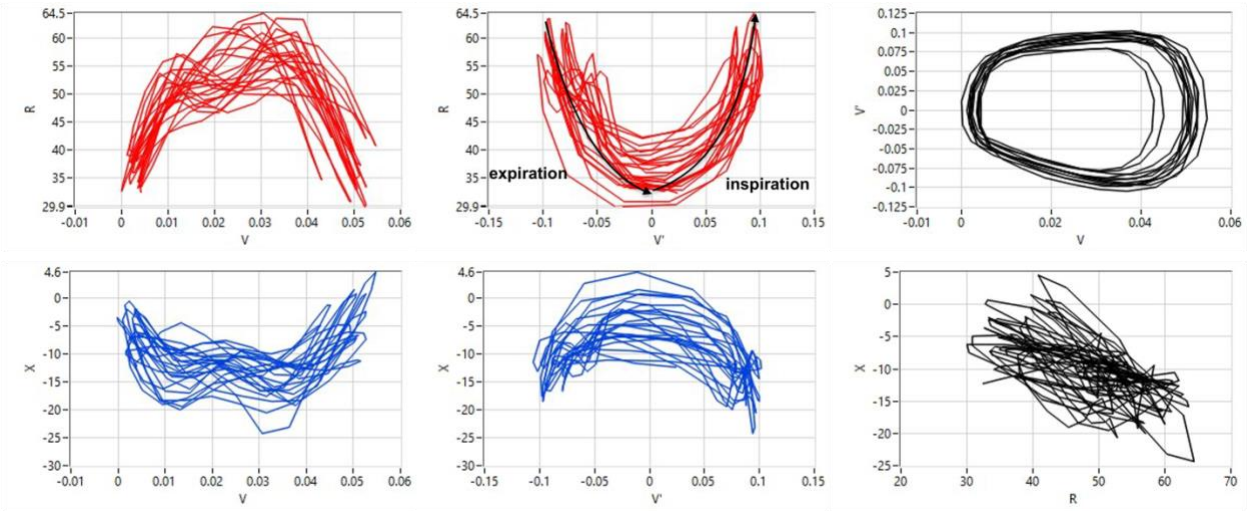

Figure 19. R-V, R-V', X-V, X-V', V'-V and X-R graphs of the fourth wave-tube segment for ID 58

The fourth wave-tube segment (Fig. 19) again shows R starting from around 30 to 35 cm H_2O/L/s and peaking around 60 to 65 cm H_2O/L/s (R-V curve), with the inspiration and expiration arms highly symmetrical in the R-V' curve.

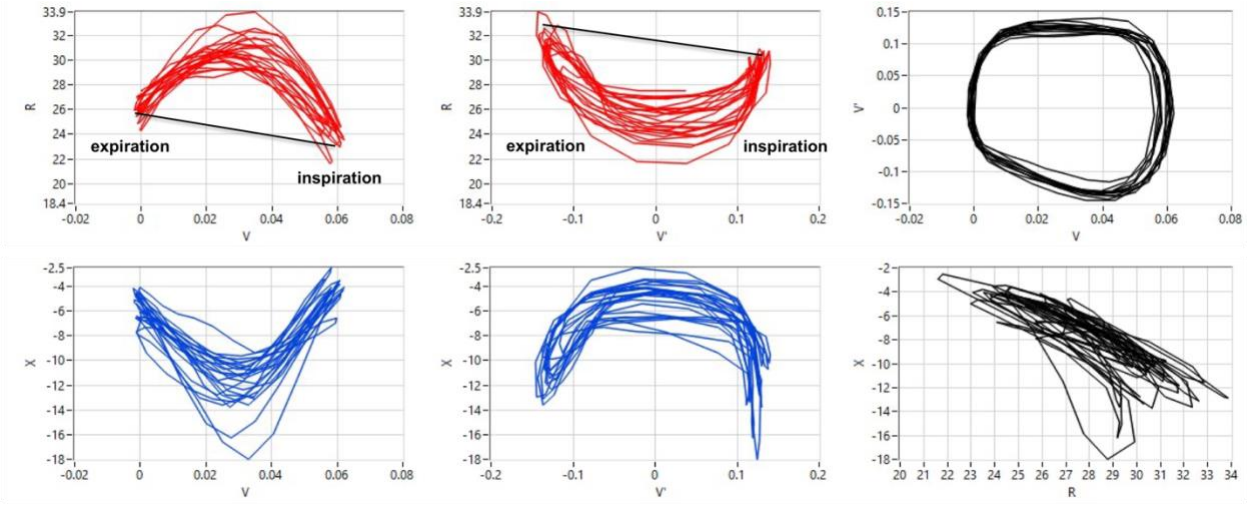

Figure 20. R-V, R-V', X-V, X-V', V'-V and X-R graphs of the first N-100 segment for ID 58

Data from the export file "Vol,Pcyl,Flow" of the N-100 were imported into the wave-tube software to generate these intra-breath graphs. In the first N-100 segment (Fig. 20), the overall level of R is lower, which is consistent with the inter-device differences in R found with the spectral recordings. R starts from around 20 to 25 cm H_2O/L/s (R-V curve) and peaks around 30 to 35 cm H_2O/L/s (R-V' curve). The increase in R is much smaller than the doubling apparent in all the wave-tube segments.

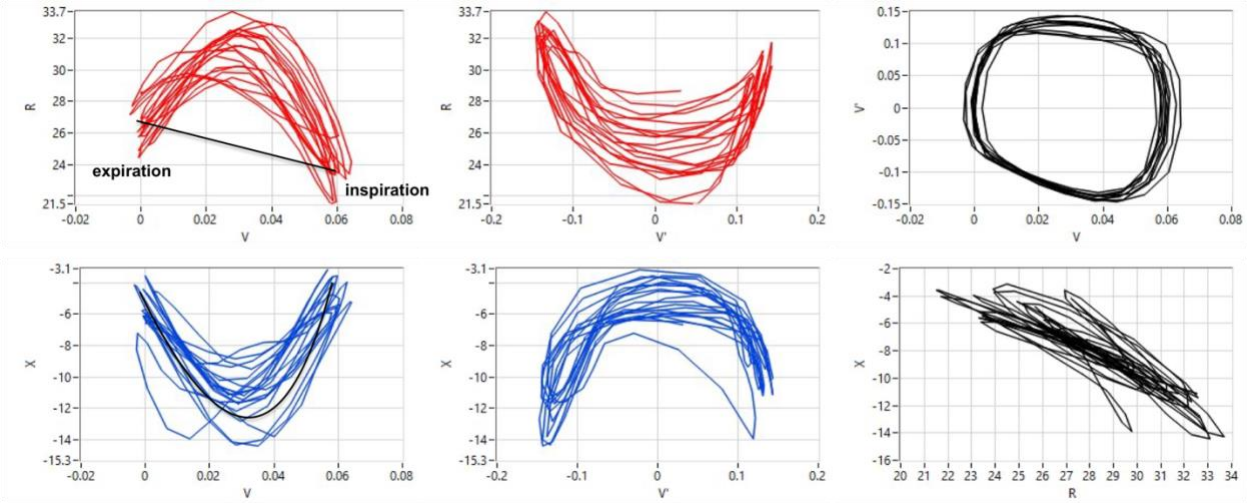

Figure 21. R-V, R-V', X-V, X-V', V'-V and X-R graphs of the second N-100 segment for ID 58

In the second tremoFlo® N-100 segment (Fig. 21), R at end-inspiration is lower than at end-expiration (R-V curve). Curiously, this trend is present in all tremoFlo® segments, but in none of the wave-tube recordings. The reactance mirrors resistance (X-V' curve).

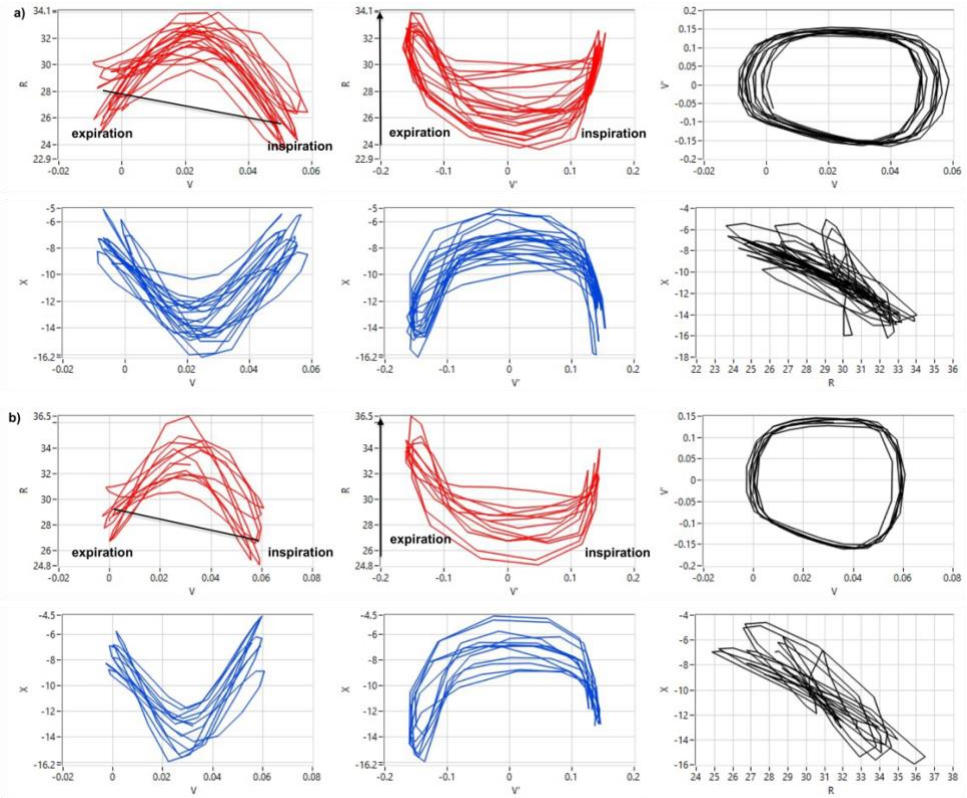

Figure 22. R-V, R-V', X-V, X-V', V'-V and X-R graphs of the a) third and b) fourth N-100 segments for ID 58

The third (Fig. 22a) and fourth segments (Fig. 22b) from the N-100 show the same patterns of an overall lower level of R, with no doubling (R-V' curves) and a consistent change occurring between end-inspiration and end-expiration (R-V curves).

Intra-breath analysis of all wave-tube segments revealed stable breathing patterns, with the same resistance at end-inspiration and end-expiration, which consistently doubled from minimum to maximum. Although the third segment showed airways at near collapse, it is a natural feature of infant breathing that is not excluded from analysis.

Table 10 shows intra-breath indices calculated from all 4 segments of the wave-tube and tremoFlo® N-100 for ID 58. There are large differences in total respiratory cycle time, tidal volume and respiratory rate between devices. The infant was breathing more slowly when recording with the wave-tube.

All the resistance indices (R_{eE}, R_{eI}, $R_{eE} - R_{eI}$, $R_{eE} - R_{eI}/V_T$, $R_{max,E}$, $R_{min,E}$, $R_{max,I}$, $R_{min,I}$, R_{mean}) had discrepancies between devices. Differences in resistance at end-expiration (R_{eE}) and end-inspiration (R_{eI}) and mean resistance during the breathing cycle (R_{mean}) were similar to the differences observed in spectral measurements from both devices. Maximum resistance measured by the N-100 were consistently about half of those measured by the wave-tube for both expiration and inspiration, demonstrating the overall lower level of R measured by the N-100.

Just like the spectral measurements, reactance recorded for the intra-breath measurements were similar in the wave-tube and the N-100 (X_{eE}, X_{eI}, $X_{eE} - X_{eI}$, $X_{eE} - X_{eI}/V_T$, $X_{max,E}$, $X_{min,E}$, $X_{max,I}$, $X_{min,I}$, X_{mean}).

Table 10. Mean ± SD intra-breath data at 16 Hz from wave-tube and tremoFlo® N-100 in infant ID 58 (T_{tot} = total respiratory cycle time; V_T = tidal volume; RR = respiratory rate; R_{eE} = resistance at end-expiration; R_{eI} = resistance at end-inspiration; R_{mean} = mean resistance during breathing cycle; X_{eE} = reactance at end-expiration; X_{eI} = reactance at end-inspiration; X_{mean} = mean reactance during breathing cycle)

	wave-tube	**tremoFlo**		**wave-tube**	**tremoFlo**
$\mathbf{V_T}$	0.046 ± 0.00	0.060 ± 0.00	$\mathbf{T_{tot}}$	1.57 ± 0.13	1.23 ± 0.10
RR	38.36 ± 3.18	49.16 ± 4.11			
$\mathbf{R_{eE}}$	35.70 ± 2.82	26.96 ± 1.56	$\mathbf{X_{eE}}$	-4.35 ± 2.88	-6.51 ±1.55
$\mathbf{R_{eI}}$	37.10 ± 5.31	24.89 ± 1.66	$\mathbf{X_{eI}}$	-2.86 ± 4.57	-5.70 ± 1.81
$\mathbf{R_{eE} - R_{eI}}$	-1.39 ± 5.92	2.07 ± 1.85	$\mathbf{X_{eE} - X_{eI}}$	-1.50 ± 5.04	-0.81 ± 1.77
$\mathbf{R_{eE} - R_{eI}/V_T}$	-29.89 ± 125.85	34.91 ± 31.05	$\mathbf{X_{eE} - X_{eI}/V_T}$	-32.96 ± 106.24	-13.68 ± 29.93
$\mathbf{R_{max,E}}$	57.86 ± 2.86	32.88 ± 1.39	$\mathbf{X_{max,E}}$	-1.33 ± 3.19	-5.54 ± 1.65
$\mathbf{R_{min,E}}$	34.31 ± 2.61	25.31 ± 1.60	$\mathbf{X_{min,E}}$	-14.04 ± 2.77	-13.31 ± 1.76
$\mathbf{R_{max,I}}$	60.56 ± 4.06	30.95 ± 1.19	$\mathbf{X_{max,I}}$	-1.49 ± 3.69	-5.31 ± 1.54
$\mathbf{R_{min,I}}$	33.80 ± 2.52	24.52 ± 1.57	$\mathbf{X_{min,I}}$	-19.34 ± 2.43	-12.25 ± 2.03
$\mathbf{R_{mean}}$	48.65 ± 1.75	28.85 ± 1.00	$\mathbf{X_{mean}}$	-9.92 ± 1.26	-9.13 ± 1.25

4.2.3 Quality Control

Internal quality control software of the tremoFlo® automatically excluded measurements with insufficient data for analysis. Since all coherence values satisfied the pre-set threshold of more than 0.5, further measurements, or portions thereof, containing breath holds, cries or irregular breathing, were excluded in an initial data review to obtain the prerequisite CV of 15% or lower within the program. Doing so left some participants with 3 valid measurements. For the remaining participants, the 3 measurements that had the closest values of R7, X7, R16, X16 and AX, listed in priority sequence, were included in participant means. If the 3 selected values were obtained in various sleep positions, they were analyzed separately and in combination. Since there were no apparent differences between the values obtained in each sleep position, all 3 measurements were used in combination to derive the mean for that subject.

In the second part of the study, a few, longer recordings of a maximum of 120 seconds were obtained, while the facemask remained in place. Recording segments containing zero-flow and pauses in volume simultaneously were excluded because they represent breath holds, cries or irregular breathing[25]. Manifesting as large impedances at zero-flow, swallows and transient airway occlusions were also excluded. Segments with negative resistance were removed, as they indicate noise artefacts like coughs[25]. Facemask leak was the most common issue, indicated by sudden spikes in the resistance and pressure signals, with very subtle changes in the flow–time and volume–time signals[25]. Anonymized wave-tube recordings were sent to Zoltan Hantos for analysis and RCL model-fitting.

4.2.4 Questionnaires

All parents who completed the questionnaire (Appendix A, Fig. A1) at the end of each visit either agreed or strongly agreed that testing was comfortable for the baby, testing duration was acceptable and that they would allow their baby to be tested again in the future. The operator questionnaire (Appendix A, Fig. A2) usually agreed that the setup and calibration were easy. The device became easier to manipulate once the generic support arm was replaced with the manufacturer's in-house support arm. Software issues were relayed to the manufacturer and infant tolerance and seal depended on the infant, not the device itself.

Chapter 5: Discussion

5.1 Study Implications

5.1.1 Impedance

All infants from the first part of the study were within the reproducibility threshold, except ID 19. Although asleep, he was tested in a more upright position compared with the rest of the infants, which may explain the high coefficient of variation (CV). There may have been less upward pressure of the abdominal contents, especially post-feed, invalidating that test. Additionally, all infants reached resonant frequency (f_{res}), except ID 36. At seven weeks old, she was younger and smaller than the rest of the infants. Inertance is deemed negligible in infants due to their small lungs, which may explain the lack of f_{res}. Meanwhile, the other infants aged 10 to 11 weeks may have undergone sufficient lung growth to display inertance and reach f_{res}.

The improved coherence (COH) during sleep may be attributed to the more regular breathing pattern of sleep, making infants less likely to react to the placement of the facemask. The improved CV with the addition of the bias flow can be explained by the flushing of equipment dead space, bringing in a fresh supply of medical-grade air to prevent CO_2 rebreathing. There was no correlation between impedance and length, weight or sex. This is in contrast with Gray et al. (2015)[52], who used the wave-tube in healthy African infants without sedation aged 5 to 11 weeks old. Length was positively associated with R_{rs}, C_{rs} and f_{res}, whereas weight was positively associated with R_{rs}[52]. Male gender was associated with increased R_{rs}, decreased Crs and a slightly higher f_{res}[52]. Another study[51] from the same team found birth weight to be associated with lower C_{rs} and male gender with increased R_{rs} and decreased C_{rs}. Our results matched those of Klinger et al. (2020)[60], who used the modified tremoFlo® C-100 in healthy, term neonates without sedation on the first three days of life. They did not find any strong correlations between birth weight or length and R, X or AX[60].

In the second part of the study, all subjects were within the reproducibility threshold using the wave-tube. However, using the tremoFlo®, ID 86 had a COH of 0.41 and ID 84 had a CV of 18.7%, both very close to this study's cut-offs of 0.50 and 15%, respectively. Currently, it is not known whether COH is a valid measure of reproducibility, with increasing support for CV. The latest ERS guidelines reported a CV of 15% or lower for children indicates sufficient reproducibility, although they noted the lack of evidence to support this cut-off[25]. Yet, they maintained using an arbitrary threshold accomplishes the purpose of CV, which is to exclude outliers by forcing the selection of measurements close to each other. Exclusion of extreme outliers is crucial in infants, as the nasal passages and upper airways are dominant areas of resistance and are included in their measurements[84]. However, infants may have more natural

variability in respiratory mechanics[85] than children, warranting a higher threshold. This may explain why Klinger et al. (2020)[60] opted for a higher CV cut-off of 25% based on preliminary results using the modified tremoFlo® C-100. Another recent study[86] using the wave-tube had similar findings and recommended more permissive reproducibility criteria. A threshold of 20% may be small enough to exclude extreme outliers, yet large enough to be supported by current evidence.

All infants reached f_{res}, except ID 86 with both devices and 84 with tremoFlo® only. From the first part of the study, ID 36 did not attain f_{res} due to being younger and smaller. This can be reasonably eliminated as a potential reason for ID 86, since he was at the other extreme, weighing 5.9 kg at 10 weeks old. He did exhibit low compliance and large inhomogeneity, leading to the lack of f_{res}. Although X_{rs} for ID 84 did not cross the x-axis with the tremoFlo®, the wave-tube measured f_{res} at 29 Hz, more than 10 Hz higher than the other infants. Unlike the other infants, he was tested in his parent's arms, which may have affected the quality of measurements. Yet, CV for wave-tube met the threshold, indicating sufficient quality. Although he was the same height as ID 86, he weighed a kilogram less. Being leaner may have had the same effect as having smaller lungs with high compliance, thus increasing f_{res}.

Although the sample size was small, X37 showed excellent reliability while X19, X29, R7-19 and AX showed modest reliability based on intraclass correlation coefficient. For these variables, measurement error had minimal effect on the ability of the device to distinguish subjects. Interestingly, the UAB team found the modified C-100 could distinguish between healthy and TTN neonates based on all X_{rs} recorded at 17 to 37 Hz[60], the same variables that were cautiously assessed as reliable in this study.

Resistance measured by the tremoFlo® was consistently lower than the wave-tube at all frequencies. Although filter impedance was incorporated into the N-100 calibration, the facemask impedance was considered a static part of the respiratory system, unlike the wave-tube. Test measurements examining the impact of the different approach to facemask impedance indicated the lack of correction for mask impedance to be only partially responsible for this systematic bias. Another possible source of error may be the three-point model used in the dynamic calibration of the N-100. The model may not adequately simulate resistance changes during tidal breathing.

Resistance measured by the modified tremoFlo® C-100 in healthy infants on postnatal day 1 was visually estimated based on Figure 3a of the UAB study[60]. Mean resistance at all frequencies using the N-100 was higher than the modified C-100, especially at higher frequencies (N-100 vs. C-100; R7 = 35.5 vs. 30 cm H_2O/L/s; R13 = 28.7 vs. 23.8 cm H_2O/L/s, R19 = 26.5 vs. 10 cm H_2O/L/s, R29 = 25.4 vs. 11 cm H_2O/L/s, R37 = 25.5 vs. 15 cm H_2O/L/s). This was expected as the calibration test loads of 2 and 15 cm H_2O/L/s used in that study enabled accurate impedance measurements within that range only. Errors potentially present at the high impedance of infants could not be compensated. The N-100 used not only

higher test loads of 25 and 90 cm H_2O/L/s, but also oscillations with higher amplitudes and sensors with modified gain and zero offset to improve accuracy.

Mean resistance were reported[60] to be similar to those made by the wave-tube on the first three days of life[49], although it was acknowledged that the total tidal volume of the infant was not captured, as the dead space of the filter and mask were not flushed by a bias flow. The authors[60] noted their mean resistance was lower than those reported by Gray et al.[26], attributing the discrepancy to the difference in age of the study population in the latter study. Gray et al.[26] tested 6- to 10-week-old infants with the wave-tube from 8 to 48 Hz. The resistance we measured with the wave-tube in similar-aged infants was close to their wave-tube measurements (mean ± SD; R7 = 51.0 ± 7.3 vs. R8 = 62.2 ± 22.1 cm H_2O/L/s; R13 = 49.3 ± 16.2 vs. R12 = 58.9 ± 21.7 cm H_2O/L/s; R19 = 44.3 ± 11.7 vs. R16 = 54.6 ± 20.9 cm H_2O/L/s). Wave-tube resistance after model-fitting in this study were also similar[26] (median [IQR 25%; 75%] R = 40.7 [37.4; 47.4] vs. 45.0 [37.5; 55.8] cm H_2O/L/s).

Reactance and f_{res} measurements from each device appeared to be in close agreement. Inflating the air cushion rim of the mask may have helped reduce upper airway shunt to the more compliant structures of the upper airways, like the cheeks. In adults and children, cheek support is thought to partially correct for this upper airway artefact, but since subject comprehension is not feasible in infants, inflating the mask rim may be an alternate method to account for shunt compliance.

Reactance measured by the modified tremoFlo® C-100 in healthy infants on postnatal day 1 was visually estimated based on Figure 3a of the UAB study[60]. Mean reactance at all frequencies using the N-100 was less negative than the modified tremoFlo® C-100[60] (N-100 vs. C-100; X7 = -20.1 vs. -44 cm H_2O/L/s; X13 = -12.4 vs. -32 cm H_2O/L/s, X19 = -7.2 vs. -20 cm H_2O/L/s, X29 = -3.2 vs. -10 cm H_2O/L/s, X37 = 0.28 vs. -7 cm H_2O/L/s). In addition to the modifications lending the N-100 more accuracy, these differences may also be explained by the difference in the study population age between the studies. The reactance we measured with the wave-tube matched those of Gray et al.[26] in similar-aged infants (mean ± SD; X7 = -20.4 ± 11.2 vs. X8 = -22.4 ± 12.2 cm H_2O/L/s; X13 = -13.1 ± 9.0 vs. X12 = -15.5 ± 8.7 cm H_2O/L/s; X19 = -7.6 ± 10.7 vs. X16 = -9.1 ± 7.2 cm H_2O/L/s).

Initially, the difference between resistance at 7 and 19 Hz was used to characterize the frequency dependence of resistance. However, R7-29 may better represent this dependence in infants because the higher upper limit of 29 Hz is more consistent with the higher pitch. Indeed, values from each device for R7-29 agreed more closely than R7-19. A recent study[86] using the wave-tube reported a mean R8-32 of 18.6 ± 7.3 SD cm H_2O/L/s on the first five days of life, while we found mean R7-29 to be 8.6 ± 1.6 SD cm H_2O/L/s in 7 to 11-week-old infants. Even though frequency dependence of R_{rs} becomes less evident with increasing age[29–33], it cannot be said if that was the case here due to the small study population.

Finally, reactance area below f_{res} (AX) showed the largest measurement error. AX is reported in oscillometry studies because it has been shown to be higher in asthma than healthy controls in the adult population[19,38,39]. However, the ability of OSC to distinguish between health and asthma in children has shown mixed results[40–43] and its utility in infants is not currently known. The UAB team reported AX ranging from 624 to 765 cm H_2O/L on the first three days of life[60], while the N-100 measurements of this study ranged from 174 to 275 cm H_2O/L. This follows from the mean reactance at all frequencies using the modified tremoFlo® C-100[60] being much more negative than the N-100.

5.1.2 Intra-Breath Tracking

Intra-breath tracking at a single frequency allows closer examination of inspiration and expiration and the resulting changes in impedance. Changes in X_{rs} are especially useful to detect expiratory flow limitation and was found to discern healthy preschoolers from those with recurrent wheeze[37,57]. Intra-breath analysis of wave-tube measurements at 16 Hz was shown to identify healthy six-week-old infants at risk of developing LRTI, wheezing or severe illness at the age of one based on volume dependence of R_{rs} and X_{rs}, creating the potential for monitoring and early intervention[50].

The 16 Hz curves of ID 58 demonstrated a consistent trend in the N-100 recordings of a lower end-inspiration R than end-expiration. Curiously, this trend is present in all tremoFlo® segments, but in none of the wave-tube recordings. Modifications to the technical settings did not resolve this difference. Furthermore, all wave-tube segments consistently showed resistance as doubling, whereas the N-100 had an increase of only about 10 cm H_2O/L/s. The overall level of R is lower in the N-100, which is consistent with the inter-device differences in R found with the spectral recordings.

The mean intra-breath indices from all segments for each device unexpectedly revealed large differences in tidal volume (V_T) and respiratory rate (RR) between measurements from each device, which led to the large difference in total respiratory cycle time (T_{tot}). The infant was breathing more slowly when recording with the wave-tube, perhaps due to it being the second device tested, giving the infant time to get more settled. It supports the recommendation of longer data acquisition duration, as infant breathing has inherent variability that can only be captured with 60 to 120 second recordings. Longer measurements demonstrate the baseline for each infant and provide context permitting the reliable analysis of more transient changes in impedance from swallows, sighs and other sources.

Yet, breathing rate does not explain the discrepancies in all resistance indices between devices. Resistance at end-expiration (R_{eE}) and end-inspiration (R_{eI}) and mean resistance during the breathing cycle (R_{mean}) matched the differences observed in the spectral measurements from both devices. Maximum resistance demonstrated the inter-device difference most clearly, with N-100 measurements being consistently about half of wave-tube measurements for both expiration and inspiration. Since the minimum and maximum values that can be reliably measured by the device is determined by measuring and fitting

the gain and zero offset errors to the pressure and flow sensors, a potential solution could be to refit the N-100's sensors using a stable flow bench system.

The systematic underestimation of resistance by the tremoFlo® may resolve after calibrating for mask impedance and modifying the resistance component of the three-point model. Just like the spectral measurements, the N-100 measured intra-breath reactance adequately when compared with the wave-tube, signifying sufficient simulation of changes in reactance during tidal breathing.

5.1.3 Testing Protocol

The small number of infants from whom reliable data were obtained with both devices highlights the importance of an exceptionally positive environmental setting conducive to testing infants, free of time constraints, as well as a dedicated, consistent team of more than one individual. Several parents scheduled their clinic visits to be right after the routine two-month pediatric checkup for their infants, lessening patient burden. Many, though not all, guardians were willing to remain for up to four hours if needed, trying to put their infants to sleep. However, the greatest difficulty encountered in this study was achieving the appropriate sleep state to enable testing. Once all four recordings were obtained, there was understandably a sense of urgency to leave as soon as the test was over. Subsequently, although four recordings were obtained for a majority of the infants, measurements from only four infants had a minimum of three 10- to 30-second segments to make inter-device comparisons of spectral data. All four recordings were valid for only ID 58, who, interestingly, was the quickest to test, as the appointment was booked during her routine feed and nap time. However, not all infants establish a sleep schedule at this age and some infants who did were so stimulated by the new environment, they stayed awake, despite being visibly tired.

After consulting with other research groups, the differences in study protocols were uncovered. In the wave-tube study from Hungary[49], the mother and neonate were discharged from the maternity ward three days after delivery as per hospital protocol. Their 72-hour in-patient stay provided ample time for the research group to not only achieve the appropriate sleep state, but also to verify the validity of all the recordings and repeat tests if need be. With a dedicated team for the study, they were able to return the next day in some cases, enabling the 79% success rate in testing neonates on the first three days of life, as well as infants a few weeks old[49].

In the South African Drakenstein Child Health wave-tube studies[50], over 700 infants in the same age group as this study were tested. Like this study, subjects were compensated for travel, but transport was also provided for some to travel to the test site. A common reason for decline in this study was access to a car, which was driven by a working parent who would have to take time off work to participate in the study. Since stay-at-home moms were part of the cultural norm in South Africa, they were willing to stay at the hospital for as long as required. There was no rush as they sat in a room adjacent to the test room, with the TV on for entertainment. If an infant woke up mid-test, they were brought to their mother, who would then

try to put them back to sleep, even if it took several hours. This allowed the research team to derive reliable, valid data from not only infants, but also toddlers of up to two years old with a 79% success rate.

Still, strategies were implemented to adjust the original protocol, like asking parents to avoid allowing infants to sleep in the car on the way to the hospital, a recommendation from the South African studies[26,50–52]. This was not always feasible, especially for those travelling into the city from the suburbs. Recording the infant's height and weight was moved from the beginning to the end of the visit to create a calm and comfortable pre-test atmosphere to encourage post-feed sleep. It was also found that white noise for colicky babies was effective in achieving the sleep state required for testing. Modifications were made to the light displays on the main unit of the tremoFlo® by covering them with cotton pads to keep the environment dark.

This study found that laying supine on the bed was the optimal sleep position to obtain valid results from infants. Some infants did not like sleeping on their backs, in which case they were placed in the parents' arms, making sure to keep them horizontal and avoid neck flexion. Although not ideal, valid measurements were also obtained in that position. On the other hand, testing in the stroller, even using a shoulder roll for neck extension, did not provide adequate measurements, likely because the infant was at a slight incline, not completely horizontal. This may have led to forward slouching, which could compress the abdomen and move its contents upwards into the thorax, causing some airway narrowing and decreased lung volume.

Initially, in the absence of a bias flow of medical-grade air, it was observed that infants woke up as soon as testing was initiated and remained fairly agitated. This may explain why the UAB team[60,61], who also did not utilize a bias flow, took measurements of eight seconds only, which is the lower end of the range of eight to 12 seconds used in the initial part of this study. Once a bias flow of 2 L/min was implemented, as reported in the Drakenstein studies[26,50–52], the infants remained asleep, showed no signs of agitation and appeared to breathe more comfortably. It allowed an increase in measurement duration to 60 seconds. Finally, on the advice of Zoltan Hantos in December 2021, the measurement duration was extended to 120 seconds, without removing the facemask, for all the external validation tests. This was found to be more practical as it minimized any disturbance to the sleeping infant caused by the removal and replacement of the facemask between multiple, shorter measurements.

5.2 Strengths of Current Study

5.2.1 Bias Flow

Using a bias flow ensured equipment dead space was not a confounding variable when measuring impedance. The UAB studies[60,61] conceded that the total tidal volume of the infant was not captured, as the dead space of the filter and mask were not flushed by a bias flow. According to the ERS guidelines[25], given

a choice between minimizing resistance at the expense of increased equipment dead space or minimizing equipment dead space at the expense of increased resistance, it is preferable to minimize resistance, since the additional dead space can be easily flushed out by the bias flow. To minimize resistance, several filters were tested and the one with the lowest resistance was selected. For the same reason, the bias flow line with the lowest diameter was chosen.

5.2.2 Replicates and Duration of Data Acquisition

The UAB team[60,61] performed up to five measurements of eight seconds, using the mean data of only two artefact-free recordings for analysis. While no difference was found between mean values obtained with two, compared with three or more, measurements in adults[87], no such evidence exists for children or infants[25]. Furthermore, a short duration of five to eight seconds is recommended for low-frequency OSC measured during apneic periods to reflect a reasonable breath-hold time interval[25]. However, a longer duration of 30 to 60 seconds is recommended for quietly breathing sleeping infants to maximize the number of breath cycles recorded[25].

Consequently, this study used longer measurements lasting 120 seconds, from which at least three steady-state 10 to 30-second artefact-free segments were used to derive mean values. In a recent study[86], the most stable spectral values were obtained for R and |Z8| from 90-second recordings. Longer measurement durations may provide more accurate data by capturing a larger number of breath cycles. Additional accuracy is conferred by keeping the facemask on the infant throughout the entire duration of the test, instead of constantly removing and repositioning the mask in between shorter measurements. The latter practice decreases accuracy by potentially changing the infant's breathing pattern or sleep stage due to the recurring facial nerve stimulation[88]. The redesigned N-100 isolated the vibrations of the main unit from the sleeping infant, making it more feasible to capture these longer, more accurate recordings.

5.2.3 tremoFlo® N-100 Calibration

Another strength of this study was the use of both static and dynamic calibration. Other commercial oscillometers only use a low, static reference impedance for calibration and a rudimentary approach to correct for the impedance of the filter and facemask[76]. However, it was found that systematic errors in Z_{rs} measurements remain in the system, especially at the high impedance values of infants[76].

The manufacturers performed static and dynamic calibrations for each device. Wave-tube calibration is outlined elsewhere[49]. For the tremoFlo®, static calibration accounted for sensor gain and off-set errors, whereas dynamic calibration accounted for any errors remaining in the system by using a three-point lung model simulating Z_{rs} changes during tidal breathing[76].

The test loads used to calibrate the N-100 were higher than those of the modified C-100. This improved accuracy by expanding the range of impedance values that can be accurately measured with the device.

When the three-point model was analyzed with the wave-tube software, it was found to be leaky. The model was taken apart and reassembled meticulously to ensure proper tight sealing at all points of potential leakage. After reanalysis with the wave-tube software confirmed the absence of leaks, the model was then connected to the tremoFlo® N-100 to recalibrate the device.

5.3 Limitations of Current Study

5.3.1 Age and Study Setting

The target age of the study population was chosen as two to three months old, with the assumption that parents could book the test on the same day as the recommended two-month pediatric checkup, reducing the burden of multiple visits. Following the success of the Drakenstein studies[26,50–52] testing infants at this age, it was thought they would naturally sleep. However, the greatest difficulty encountered in this study was achieving the appropriate sleep state to enable testing. Since even two-month-olds appear to be significantly aware of their surroundings and too curious about their new environment to fall asleep, testing infants in the first month of life may be more convenient because they remain in natural sleep for substantially longer periods of time.

As mentioned previously, it may not be age, but the study setting that led to the small sample size of this study. Based on the South African Drakenstein Child Health wave-tube studies[50], even infants of up to two years of age can be tested, given an environment favourable for testing non-cooperative subjects that is free of time constraints. A consistent research team dedicated to the study would permit continuous, uninterrupted recruitment, followed by a constant flow of enrolment. A regular stream of subjects, combined with having the same set of people conducting the tests would be beneficial because as they test more infants, they would gain experience and remember which methods were the most effective for reliable data collection and which approach may be less ideal. They would be better able to improve the protocol, resolve issues and learn from the initial tests.

It should be noted that pandemic-related events, such as the emergence of new variants hampering a steady flow of recruitment and enrolment, were beyond our control. Furthermore, we were unable to start making inter-device comparisons until the two-week quarantine travel restrictions were lifted, allowing Dr. Hantos to bring the wave-tube to Montreal in December 2021. That left around six months of this two-year study to obtain measurements from both devices.

5.3.2 tremoFlo® N-100 software

A dark room was essential to helping the infant fall asleep. Although the wave-tube software had the option of a dark background to minimize glare from the laptop screen, the tremoFlo® software lacked such an option. Subsequently, a test room with a window permitting natural light would have been more useful to visually confirm the infant is in deep, non-REM sleep.

The latest guidelines[25] recommend the use of three replicates at the lowest frequency to compute CV of R_{rs}, in this case, R7. The standard deviation (SD) of R7 data is compared to the mean to detect potential outliers. However, once the switch to 120-second recordings was made, it was found that the tremoFlo® software cannot calculate SD, and thus CV, based on R7 data from one long recording, it can only do so with multiple, shorter recordings. The tremoFlo® software also lacked the ability to split one long recording into multiple, shorter recordings. The absence of these features, together with the limited types of raw data export files available from the software, rendered manual calculation of CV very time and labour intensive.

The "Detailed Measurements" export file contained the means of R_{rs} at each frequency, with the option to export means including or excluding segments with artefacts. But it did not contain the raw data from which the mean and SD could be calculated. The raw values of R7 recorded over time within one recording were in the "Timecourse" export file, but this file type did not have the option to exclude the segments with artefacts. Since it contained values from the entire recording, the timecourse view on the program showing the excluded artefact-containing segments had to be used in conjunction with the export file to manually determine the exact times at which each excluded artefact-containing segment started and ended.

This in itself was not simple either, as the software lacked an efficient way to determine the start and stop times of each excluded segment. The only way to derive this information was to carefully hover the mouse over each artefact-containing segment until it was above the exact point at which the exclusion window started and ended. After noting down the excluded time intervals, each of them was then marked on the "Timecourse" export file. Finally, the remaining artefact-free segments were selected to calculate SD.

Moreover, it was noted at the very beginning of the study that excluding segments within the program caused it to lag significantly until it froze, after which the program needed to be rebooted multiple times. The same also occurred when the height and weight of the infant needed editing. Since they were mandatory fields with conditional ranges, when a new record was created for an infant at the beginning of the visit, default values of 50 cm and 5 kg were entered so as to get to the testing screen. After the test, once the height and weight were measured, editing the patient entry caused more lag and freezing.

Finally, real-time view and analysis of impedance, like in the wave-tube, would be immensely helpful in identifying leaks, since they appear as sudden large decreases in impedance–time signals, but are too subtle to detect in the flow–time and volume–time signals, which are the ones displayed in real-time by the tremoFlo®. Furthermore, leaving the impedance analysis until after the recording is terminated caused the turnaround time to start the next recording to be inefficiently longer using 120-second recordings, compared with those of 8 to 12 seconds. This increased the chance of the infant waking up in the meantime.

It did not present a problem when the tremoFlo® was the second device to be tested, but it resulted in failing to obtain any wave-tube measurements when the tremoFlo® was tested first. This was the case for both infants who were tested with only one device.

5.3.3 tremoFlo® N-100 hardware

The support arm initially provided (Manfrotto, Videndum Media Solutions©, Italy) was originally a Photo Variable Friction Arm designed for photography. It was unwieldy, not user-friendly and a ball bearing broke, making the base unit very unstable. During an attempt to reposition the unit, the assembly wobbled onto the bed, breaking off the tubing from the adaptor with which it connected to the base unit. Thus, data from the last three infants of the internal validation portion of the study had to be discarded due to potential leaks remaining between the adaptor and the tubing.

After the tubing was repaired, THORASYS provided a support arm developed in-house specifically for use with the tremoFlo®. It was lightweight and flexible, providing a more stable support to hold the base unit. However, the base unit did not attach to the tubing adaptor as tightly as desired. Tape was wrapped around the adaptor to ensure a secure fit into the unit to prevent it from popping out during testing.

Most importantly, although the filter impedance was incorporated into the calibration, the facemask was still considered a static part of the respiratory system, unlike the wave-tube. This may partially explain the systematic bias between the devices. The three-point model used to calibrate the N-100 may also contribute to the bias. Test measurements of the three-point model with and without the facemask using both devices indicated the model may not be appropriately simulating dynamic changes in resistance.

Chapter 6: Conclusion

6.1 Study Summary

The first part of this study using only the tremoFlo® N-100 demonstrated the more regular breathing pattern during sleep improved COH, while adding a bias flow improved CV by flushing equipment dead space and supplying medical-grade air to prevent CO_2 rebreathing, maximizing comfort and reproducibility. Laying supine on the bed was the optimal test position, although if not possible, testing in the parents' arms also produced reliable data, unlike testing in a stroller. The key was to ensure the infant was kept horizontal and neck flexion was avoided. There was no correlation between impedance and height, weight or sex.

In the second part of the study, the measurement duration was extended to 120 seconds, without removing the facemask, which had an inflated air cushion rim to minimize shunt compliance. It was more practical than removing and replacing the mask between the multiple, shorter measurements of the first part. The greatest difficulty was achieving the appropriate sleep state to enable testing with both devices. As such, best practices to establish standard operating procedures are outlined in Table 11 below.

Valid spectral impedance from the wave-tube and tremoFlo® from four infants were all within the reproducibility threshold using the wave-tube, but not the N-100. However, the inherent variability of infant breathing mechanics may warrant a higher reproducibility threshold, like 20%, which is small enough to exclude extreme outliers, yet large enough to be supported by current evidence.

The small sample size of inter-device comparison highlights the importance of an exceptionally favourable environmental setting conducive to testing infants, free of time constraints, as well as a dedicated, consistent team of more than one person.

Due to the small sample size, results should be cautiously interpreted. Reliability based on intraclass correlation coefficient showed X37 had excellent reliability, while X19, X29, R7-19 and AX had modest reliability. Although the Bland-Altman plots revealed an outlier, every datapoint was situated within the 95% limits of agreement interval, indicating close agreement. However, normal distribution of the mean difference and SD of differences could not be determined due to the small study population. Resistance measured by the tremoFlo® was consistently lower than that measured by the wave-tube at all frequencies, indicating bias. On the other hand, the mean differences in reactance and f_{res} were very close to zero, indicating small measurement errors and close agreement. Mean difference of R7-29 was closer to zero than R7-19 and may better represent frequency dependence of resistance. In contrast to ICC, Bland-Altman showed AX as having the largest measurement error.

Intra-breath analysis based on four steady-state segments of 10 to 15 seconds from the wave-tube and N-100 was conducted for one infant. The infant was breathing more slowly when recording with the

wave-tube, perhaps as it was the second device tested, giving the infant time to get more settled. It supports the recommendation of longer data acquisition duration, as it captures the inherent variability of infant breathing. A consistent trend present in all tremoFlo®, but no wave-tube, recording segments was lower resistance at end-inspiration than end-expiration. Furthermore, all wave-tube segments consistently showed resistance as doubling, whereas the N-100 had a much smaller increase. Similar to the inter-device differences in the spectral recordings, intra-breath recordings systematically underestimated resistance, but adequately measured reactance. Potential solutions include refitting the gain and zero offset errors of the N-100's sensors using a stable flow bench system, correcting for mask impedance and modifying the resistance component of the three-point model.

Mean resistance at all frequencies using the N-100 was higher than the modified C-100, especially at higher frequencies. This was expected as the calibration test loads of the N-100 were higher than those of the modified C-100. This improved accuracy by expanding the range of impedance values that can be accurately measured with the device. The N-100 wave-forms also used oscillations with higher amplitudes. Mean reactance at all frequencies using the N-100 was less negative than the modified C-100. In addition to enhanced accuracy imparted by the modifications to the N-100, it may also be due to the difference in study population age. The wave-tube reactance measured in this study matched those of similar-aged infants in the Drakenstein studies.

With some modification and further validation, the tremoFlo® N-100 Airwave Oscillometry System™ is poised to become the standard device for infant oscillometry research studies and eventually routine clinical use.

Table 11. Recommended best practices to maximize success rate of reliable data collection from infants

-schedule the appointment during infant's regular naptime, if possible
-ask parents of infants to wake them up earlier than usual on the day of test
-ask parents not to let infant sleep during transport to the hospital and to keep them awake until the tester asks them to put the infant to sleep
-make sure infant's next feed falls during clinic visit to enable sleep
-record height/weight after testing to create calm, comfortable pre-test atmosphere
-play white noise for colicky babies and ensure environment is dark to encourage post-feed sleep
-ensure setting is free of time constraints and not rushed
-if infant does not manage to fall asleep, rebook for future date, with a total of three scheduled visits attempted per infant
-provide compensation for travel and time, as permitted by ethics board
-once asleep, lay infant supine on bed, with neck extended using a shoulder roll and parent supporting infant's head to face forward
-use wraps or swaddles according to infant preference
-if supine fails, attempt test while infant sleeps horizontally in parent's arms, with neck extended
-use a consistent research team dedicated to the study to learn from training and experience
-the same person should perform all the tests to keep mask pressure applied consistent
-ensure equipment calibrated and set up to begin testing as soon as infant asleep and in position

-select consumables with least resistance at the expense of increased equipment dead space
-use bias flow set to minute ventilation to flush equipment dead space
-inflate air cushion around the rim of the facemask
-record for up to 120s without removing the facemask between each measurement
-to avoid disrupting infant sleep, tester should remain as still as possible, with no distractions, solely focussed on retaining seal around facemask and observing the infant for eye movements
-another team member should monitor display signals in real-time to detect and inform tester about mask leaks, allowing readjustment and re-establishment of seal during the measurement

6.2 Study Significance

Improving quality control and standardizing the administration and performance of oscillometry devices will enhance the quality and utility of impedance measurements in clinical and research settings and allow oscillometry to reach its full potential in medicine[25].

With COH no longer recommended as a quality control measure, it is important to enable a quick and easy way to calculate CV, which the tremoFlo® software lacks when using a single 120-second recording for each subject, as revealed by this study. Most participants had measurements falling below the 15% CV threshold recommended for children[25]. The guidelines conceded the absence of current publications to support this cut-off[25], leading to the question of whether infant testing needs a higher CV threshold than children. Infants may have more natural variability in respiratory mechanics[85] than children. This finding in a recent study[86] prompted the authors to recommend more permissive reproducibility criteria. Because nasal passages and upper airways are dominant areas of resistance in infants, including the upper respiratory tract during testing[84] requires careful examination of its patency, as congestion may lead to extreme values of resistance and inertance[86].

The Drakenstein studies[26,50–52] with the wave-tube used a bias flow of medical-grade air, while the UAB studies[60,61] with the modified C-100® did not. This study tested infants with and without a bias flow to explore which configuration provided optimal results. Testing infants with both devices using bias flow not only improved CV by flushing out equipment dead space, but it also supplied air to prevent CO_2 rebreathing, making it much easier for the infant to breathe and allowing longer more accurate recordings. This finding supports the incorporation of a bias flow to standardize the administration of OSC devices.

Similarly, the Drakenstein studies[26,50–52] performed fewer, longer recordings with the wave-tube, while the UAB studies[60,61] performed many, shorter recordings with the modified C-100®. After trying both, this study found the longer recordings to enhance test performance with both devices. Instead of repeatedly placing and removing the facemask in between multiple, short recordings, a single longer measurement allowed the facemask to be held in place on the infant's face throughout the test duration. Doing so not only improved the likelihood of achieving a tight seal, it also greatly minimized disrupting the infant's sleep and

breathing. This finding supports the use of fewer, longer recordings to standardize the performance of OSC devices.

This study benefitted from collaborating with device manufacturers and other research groups in the field. As best practices to facilitate research in uncooperative infants were determined, modifications were made to the protocol accordingly. Anonymized data sharing with THORASYS Inc. for the tremoFlo® and Zoltan Hantos for the wave-tube ensured rigorous quality control. Regular discussions with the UAB and Drakenstein teams revealed insights from their experience, which were then incorporated into the study.

While the wave-tube was designed specifically for infant testing, the tremoFlo® was originally developed for adults and later modified for the special requirements of infants. Although the N-100 has the potential to become commercially available and part of routine pediatric respiratory clinical care eventually, this validation study using the latest OSC guidelines[25] highlights the need for a few modifications to make it comparable to the gold standard of the wave-tube. Changes to the software, hardware and protocol leading to the correct performance of lung function tests during infancy can provide invaluable information on lung growth and development, disease status and etiology, and to help clinician decision-making[22].

6.3 Future Directions and Recommendations

After neonatal lung function testing, the first month of life may present as the next ideal opportunity for oscillometry, as infants are less aware of their environment at this age, increasing the likelihood of achieving the appropriate sleep state. While some reference data exist for adults and children[19,28,31,73], infant OSC data remain sparse[9]. With further validation in larger samples, normal values could be established with the tremoFlo® N-100 in a wide range of populations using standardized specifications, protocols and signal analyses. The ERS report emphasizes the need for OSC normative values, similar to those established by the Global Lung Function Initiative for spirometry[74]. Future comparison studies with the wave-tube may also lead to the development of a correction factor for mask impedance, allowing the routine use of the N-100 using reference values derived from the wave-tube. With an accessible commercial device, longitudinal studies can be conducted in healthy infants and children to reveal changes in lung function that occur with growth and development, as well as better understand the origins of chronic adult respiratory diseases, like asthma and COPD, that have been traced back to early infancy[62,63].

The clinical relevance of infant lung function tests is to monitor disease progression over time and evaluate response to treatment using objective outcome measures[89]. Studies examining the N-100's potential to distinguish between healthy and clinical infant populations are underway[60]. Future research may focus on how lung function monitoring can improve patient management in infants with cystic fibrosis, bronchopulmonary dysplasia (BPD) and wheezing[89]. Data from eight European birth cohorts showed rapid growth in BMI during the first two years of life increases the risk of asthma up to the age of six[90]. With the N-100 specifically designed for use in the first two years of life, it is perfectly suited to investigate whether

earlier initiation of monitoring from infancy helps improve outcomes later in childhood for lung diseases, like asthma.

Studies correlating outcomes of different types of lung function tests with OSC outcomes will help determine the values of R_{rs}, X_{rs}, f_{res}, frequency dependence of R_{rs} and AX demonstrating respiratory dysfunction. Oscillometry provides an alternative method to spirometry for bronchial challenge tests. Unlike spirometry, OSC has the potential to detect mild airway hyperresponsiveness in earlier stages of disease due to its higher sensitivity to changes in the small airways. OSC indices may be more clinically useful, as some subjects reporting symptoms during the challenge test are deemed normal based on FEV1 measured by spirometry, but demonstrate changes in R_{rs} and AX measured by oscillometry that suggest airway narrowing and closure[91,92]. Thresholds established for OSC bronchial challenge testing in older children and adults currently reference the standard spirometry cut-offs. However, defining OSC-specific thresholds based on z-scores, instead of spirometry gold standards, would provide better validation. Studying bronchodilator responsiveness in infants and children using a standardized device would allow meaningful comparison between populations.

Collaboration between device manufacturers and multiple study centers to safely share data and expertise will greatly enhance current knowledge on oscillometry. The same technological advances that expanded the understanding of lung mechanics also pave the way to gain valuable insight into lung function trajectory and the development of pediatric lung diseases with the help of oscillometry.

References

1. West JB, Luks AM, eds. Mechanics of Breathing. In: *Respiratory Physiology: The Essentials*. 10th ed. Lippincott Williams & Wilkins; 2016:108-141.

2. McNulty W, Usmani OS. Techniques of assessing small airways dysfunction. *Eur Clin Respir J*. 2014;1(1):25898.

3. Ritz T, Dahme B, Dubois AB, et al. Guidelines for mechanical lung function measurements in psychophysiology. *Psychophysiology*. 2002;39(5):546-567. doi:10.1111/1469-8986.3950546

4. Neumann RP, von Ungern-Sternberg BS. The neonatal lung – physiology and ventilation. *Pediatr Anesth*. 2014;24(1):10-21. doi:10.1111/pan.12280

5. Mortola JP. Mechanical Behavior of the Respiratory Pump. In: *Respiratory Physiology of Newborn Mammals. a Comparative Perspective*. The Johns Hopkins University Press; 2001:101.

6. Mortola JP. Mechanics of Breathing. In: *Fetal and Neonatal Physiology*. Elsevier; 2017:706-713. doi:10.1016/B978-0-323-35214-7.00069-X

7. Sivieri EM, Bhutani VK. Pulmonary mechanics. In: *Manual of Neonatal Respiratory Care*. Springer; 2012:61-72.

8. Mortola JP. How to breathe? Respiratory mechanics and breathing pattern. *Respir Physiol Neurobiol*. 2019;261:48-54. doi:10.1016/j.resp.2018.12.005

9. Frey UP, Latzin P. Breathing Function in Newborn Babies. *Cotes' Lung Funct*. Published online 2020:423-434.

10. Wheeler DS, Wong HR, Zingarelli B. Pediatric Sepsis – Part I: "Children are not small adults!" *Open Inflamm J*. 2011;4:4-15. doi:10.2174/1875041901104010004

11. ERS Handbook of Respiratory Medicine 3rd Edition. European Respiratory Society Bookshop. Accessed November 10, 2020. https://www.ersbookshop.com/ers-handbook-of-respiratory-medicine-3rd-edition-456-p.asp

12. Bates JHT, Irvin CG, Farré R, Hantos Z. Oscillation Mechanics of the Respiratory System. In: *Comprehensive Physiology*. John Wiley & Sons, Ltd; 2011:1233-1272. doi:10.1002/cphy.c100058

13. Bayliss LE, Robertson GW. The Visco-Elastic Properties of the Lungs. *Q J Exp Physiol Cogn Med Sci*. 1939;29(1):27-47. doi:10.1113/expphysiol.1939.sp000792

14. McIlroy MB, Mead J, Selverstone NJ, Radford EP. Measurement of Lung Tissue Viscous Resistance Using Gases of Equal Kinematic Viscosity. *J Appl Physiol*. 1955;7(5):485-490. doi:10.1152/jappl.1955.7.5.485

15. Marshall R, Dubois AB. The measurement of the viscous resistance of the lung tissues in normal man. *Clin Sci*. 1956;15(1):161-170.

16. Bachofen H, Hildebrandt J. Area analysis of pressure-volume hysteresis in mammalian lungs. *J Appl Physiol*. 1971;30(4):493-497. doi:10.1152/jappl.1971.30.4.493

17. Mitzner W. Mechanics of the lung in the 20th century. *Compr Physiol*. 2011;1(4):2009-2027.

18. Hantos Z, Daroczy B, Suki B, Nagy S, Fredberg JJ. Input impedance and peripheral inhomogeneity of dog lungs. *J Appl Physiol*. 1992;72(1):168-178. doi:10.1152/jappl.1992.72.1.168

19. Peters U, Kaminsky DA, Bhatawadekar S, Lundblad L, Maksym GN. Chapter 3.2 - Oscillometry for Lung Function Testing. In: Ionescu C, ed. *Lung Function Testing in the 21st Century*. Academic Press; 2019:81-107. doi:10.1016/B978-0-12-814612-5.00005-1

20. Bates JH. *Lung Mechanics: An Inverse Modeling Approach*. Cambridge University Press; 2009.

21. DuBois AB, Brody AW, Lewis DH, Burgess BF. Oscillation Mechanics of Lungs and Chest in Man. *J Appl Physiol*. 1956;8(6):587-594. doi:10.1152/jappl.1956.8.6.587

22. Wilmott RW, Bush A, Deterding RR, et al. *Kendig's Disorders of the Respiratory Tract in Children*. Elsevier Health Sciences; 2018.

23. Reiterer F, Sivieri E, Abbasi S. Evaluation of bedside pulmonary function in the neonate: from the past to the future. *Pediatr Pulmonol*. 2015;50(10):1039-1050.

24. Fisher AB, DuBois AB, Hyde RW. Evaluation of the forced oscillation technique for the determination of resistance to breathing. *J Clin Invest*. 1968;47(9):2045-2057. doi:10.1172/JCI105890

25. King GG, Bates J, Berger KI, et al. Technical standards for respiratory oscillometry. *Eur Respir J*. 2020;55(2). doi:10.1183/13993003.00753-2019

26. Gray D, Czovek D, Smith E, et al. Respiratory impedance in healthy unsedated South African infants: effects of maternal smoking. *Respirology*. 2015;20:467-473.

27. Czovek D. Pulmonary Function Tests in Infants and Children. In: *Kendig's Disorders of the Respiratory Tract in Children*. Elsevier; 2019:174-211.

28. Oostveen E, Boda K, van der Grinten CP, et al. Respiratory impedance in healthy subjects: baseline values and bronchodilator response. *Eur Respir J*. 2013;42(6):1513-1523.

29. Cuijpers C, Wesseling G, Swaen G, Wouters E. Frequency dependence of oscillatory resistance in healthy primary school children. *Respiration*. 1993;60(3):149-154.

30. Hantos Z, Daroczy B, Gyurkovits K. Total respiratory impedance in healthy children. *Pediatr Pulmonol*. 1985;1(2):91-98.

31. Duiverman E, Clement J, Van de Woestijne K, Neijens H, van den Bergh A, Kerrebijn K. Forced oscillation technique. Reference values for resistance and reactance over a frequency spectrum of 2-26 Hz in healthy children aged 2.3-12.5 years. *Bull Eur Physiopathol Respir*. 1985;21(2):171-178.

32. Solymar L, Aronsson P, Bake B, Bjure J. Respiratory resistance and impedance magnitude in healthy children aged 2–18 years. *Pediatr Pulmonol*. 1985;1(3):134-140.

33. Stanescu D, Moavero N, Veriter C, Brasseur L. Frequency dependence of respiratory resistance in healthy children. *J Appl Physiol*. 1979;47(2):268-272.

34. Oostveen E, MacLeod D, Lorino H, et al. The forced oscillation technique in clinical practice: methodology, recommendations and future developments. *Eur Respir J*. 2003;22(6):1026-1041.

35. Sly PD, Hayden MJ, Peták F, Hantos Z. Measurement of low-frequency respiratory impedance in infants. *Am J Respir Crit Care Med*. 1996;154(1):161-166.

36. Hall GL, Hantos Z, Petak F, et al. Airway and respiratory tissue mechanics in normal infants. *Am J Respir Crit Care Med*. 2000;162(4):1397-1402.

37. Kaminsky DA, Simpson SJ, Berger KI, et al. Clinical significance and applications of oscillometry. *Eur Respir Rev*. 2022;31(163). doi:10.1183/16000617.0208-2021

38. Cavalcanti JV, Lopes AJ, Jansen JM, Melo PL. Detection of changes in respiratory mechanics due to increasing degrees of airway obstruction in asthma by the forced oscillation technique. *Respir Med*. 2006;100(12):2207-2219.

39. Qi GS, Zhou ZC, Gu WC, et al. Detection of the airway obstruction stage in asthma using impulse oscillometry system. *J Asthma*. 2013;50(1):45-51.

40. Kim HY, Shin YH, Jung DW, Jee HM, Park HW, Han MY. Resistance and reactance in oscillation lung function reflect basal lung function and bronchial hyperresponsiveness respectively. *Respirology*. 2009;14(7):1035-1041.

41. Hellinckx J, De Boeck K, Bande-Knops J, Van der Poel M, Demedts M. Bronchodilator response in 3-6.5 years old healthy and stable asthmatic children. *Eur Respir J*. 1998;12(2):438-443.

42. Malmberg L, Pelkonen A, Haahtela T, Turpeinen M. Exhaled nitric oxide rather than lung function distinguishes preschool children with probable asthma. *Thorax*. 2003;58(6):494-499.

43. Thamrin C, Gangell CL, Udomittipong K, et al. Assessment of bronchodilator responsiveness in preschool children using forced oscillations. *Thorax*. 2007;62(9):814-819.

44. Cauberghs M, Van de Woestijne K. Effect of upper airway shunt and series properties on respiratory impedance measurements. *J Appl Physiol*. 1989;66(5):2274-2279.

45. Desager K, Cauberghs M, Naudts J, Van de Woestijne K. Influence of upper airway shunt on total respiratory impedance in infants. *J Appl Physiol*. 1999;87(3):902-909.

46. Peslin R, Duvivier C, Didelon J, Gallina C. Respiratory impedance measured with head generator to minimize upper airway shunt. *J Appl Physiol*. 1985;59(6):1790-1795.

47. Hantos Z. Intra-breath oscillometry for assessing respiratory outcomes. *Curr Opin Physiol*. 2021;22:100441. doi:10.1016/j.cophys.2021.05.004

48. Grimby G, Takishima T, Graham W, Macklem P, Mead J. Frequency dependence of flow resistance in patients with obstructive lung disease. *J Clin Invest*. 1968;47(6):1455-1465. doi:10.1172/JCI105837

49. Hantos Z, Czövek D, Gyurkovits Z, et al. Assessment of respiratory mechanics with forced oscillations in healthy newborns. *Pediatr Pulmonol*. 2015;50(4):344-352.

50. Gray DM, Czovek D, McMillan L, et al. Intra-breath measures of respiratory mechanics in healthy African infants detect risk of respiratory illness in early life. *Eur Respir J*. 2019;53(5):1800998.

51. Gray D, Willemse L, Visagie A, et al. Determinants of early-life lung function in African infants. *Thorax*. 2017;72(5):445-450.

52. Gray D, Willemse L, Visagie A, et al. Lung function and exhaled nitric oxide in healthy unsedated A frican infants. *Respirology*. 2015;20(7):1108-1114.

53. Van de Woestijne KP, Franken H, Cauberghs M, Làndsér FJ, Clément J. A Modification of the Forced Oscillation Technique. In: Hutás I, Debreczeni LA, eds. *Respiration*. Pergamon Policy Studies on International Development. Pergamon; 1981:655-660. doi:10.1016/B978-0-08-026823-1.50083-1

54. Radics BL, Makan G, Coppens T, et al. Effect of nasal airway nonlinearities on oscillometric resistance measurements in infants. *J Appl Physiol*. 2020;129(3):591-598. doi:10.1152/japplphysiol.00128.2020

55. Franken H, Cement J, Cauberghs M, Van de Woestijne KP. Oscillating Flow of a Viscous Compressible Fluid Through a Rigid Tube: A Theoretical Model. *IEEE Trans Biomed Eng*. 1981;BME-28(5):416-420. doi:10.1109/TBME.1981.324725

56. Marchal F, Loos N, Monin P, Peslin R. Methacholine-induced volume dependence of respiratory resistance in preschool children. *Eur Respir J*. 1999;14(5):1167-1174.

57. Rigau J, Farre R, Roca J, Marco S, Herms A, Navajas D. A portable forced oscillation device for respiratory home monitoring. *Eur Respir J*. 2002;19(1):146-150.

58. tremoFlo® C-100 User Manual. Published online November 15, 2021.

59. Thorasys Thoracic Medical Systems Inc., Montreal, Canada. tremoFlo® C-100 Technical Specifications (English). Published online May 2015. Accessed February 6, 2022. https://thorasys.com/wp-content/uploads/2015/05/tremoFlo-C-100-Specifications-English-102264-Rev-2.2.pdf

60. Klinger AP, Travers CP, Martin A, et al. Non-invasive forced oscillometry to quantify respiratory mechanics in term neonates. *Pediatr Res*. 2020;88(2):293-299.

61. Travers CP, Klinger AP, Aban I, Hoover W, Carlo WA, Ambalavanan N. Noninvasive Oscillometry to Measure Pulmonary Mechanics in Preterm Infants. *Am J Respir Crit Care Med*. 2021;204(4):485-488.

62. Kabesch M. Early origins of asthma and allergy. *Mol Cell Pediatr*. 2016;3(31).

63. Stern DA, Morgan WJ, Wright AL, Guerra S, Martinez FD. Poor airway function in early infancy and lung function by age 22 years: a non-selective longitudinal cohort study. *The Lancet*. 2007;370(9589):758-764.

64. Ducharme FM, Dell SD, Radhakrishnan D. Diagnosis and management of asthma in preschoolers: A Canadian Thoracic Society and Canadian Paediatric Society position paper. *Can Respir J*. 2015;22(3):135-143.

65. Graham BL, Steenbruggen I, Miller MR, et al. Standardization of spirometry 2019 update. An official American thoracic society and European respiratory society technical statement. *Am J Respir Crit Care Med*. 2019;200(8):e70-e88.

66. Lum S, Stocks J, Castile R, Davis S. ATS/ERS statement: raised volume forced expirations in infants: guidelines for current practice. *Am J Respir Crit Care Med*. 2005;172(11):1463.

67. Willemse L, Visagie A, Jacobs CD, Zar HJ, Hall GL, Gray DM. High success rate of lung function testing in healthy, unsedated 1-and 2-year-old South African children. *Ann Am Thorac Soc*. 2016;13(11):2099-2101.

68. Lundblad LKA, Robichaud A. Oscillometry of the respiratory system: a translational opportunity not to be missed. *Am J Physiol-Lung Cell Mol Physiol*. 2021;320(6):L1038-L1056. doi:10.1152/ajplung.00222.2020

69. Evans J, Chen Y, Camp PG, Bowie DM, McRae L. Estimating the prevalence of COPD in Canada: Reported diagnosis versus measured airflow obstructio. *Health Rep*. 2014;25(82):11.

70. *Global Initiative for Asthma. Global Strategy for Asthma Management and Prevention*.; 2021. http://www.ginasthma.org/

71. Lougheed MD, Lemiere C, Ducharme FM. Canadian Thoracic Society 2012 guideline update: Diagnosis and management of asthma in preschoolers, children and adults. *Can Respir J*. 2012;19:127-164.

72. Wouters E, Polko A, Schouten H, Visser B. Contribution of impedance measurement of the respiratory system to bronchial challenge tests. *J Asthma*. 1988;25(5):259-267.

73. Clement J, Landser F, Van de Woestijne K. Total resistance and reactance in patients with respiratory complaints with and without airways obstruction. *Chest*. 1983;83(2):215-220.

74. Quanjer PH, Stanojevic S, Cole TJ, et al. Multi-ethnic reference values for spirometry for the 3–95-yr age range: the global lung function 2012 equations. Published online 2012.

75. Lum S, Hoo A, Hulskamp G, Wade A, Stocks J. Potential misinterpretation of infant lung function unless prospective healthy controls are studied. *Pediatr Pulmonol*. 2010;45(9):906-913.

76. Sly PD, Shackleton C, Czovek D, Hantos Z. Systematic error in respiratory impedance using commercial equipment calibrated according to the manufacturer's instructions. *Am J Respir Crit Care Med*. 2018;197(4):532-534.

77. Walter SD, Eliasziw M, Donner A. Sample size and optimal designs for reliability studies. *Stat Med*. 1998;17(1):101-110. doi:10.1002/(SICI)1097-0258(19980115)17:1<101::AID-SIM727>3.0.CO;2-E

78. Arifin WN. Sample size calculator. Published 2022. Accessed February 15, 2022. https://wnarifin.github.io/ssc/ssicc.html

79. Bolton DP, Herman S. Ventilation and sleep state in the new-born. *J Physiol*. 1974;240(1):67.

80. Frerichs I, Schiffmann H, Oehler R, et al. Distribution of lung ventilation in spontaneously breathing neonates lying in different body positions. *Intensive Care Med*. 2003;29(5):787-794.

81. Desager K, Buhr W, Willemen M, et al. Measurement of total respiratory impedance in infants by the forced oscillation technique. *J Appl Physiol*. 1991;71(2):770-776.

82. de Vet HC, Terwee CB, Knol DL, Bouter LM. When to use agreement versus reliability measures. *J Clin Epidemiol*. 2006;59(10):1033-1039.

83. Bland JM, Altman DG. Measuring agreement in method comparison studies. *Stat Methods Med Res*. 1999;8(2):135-160.

84. Solow B, Peitersen B. Nasal airway resistance in the newborn. *Rhinology*. 1991;29(1):27-33.

85. Beydon N, Davis SD, Lombardi E, et al. An official American Thoracic Society/European Respiratory Society statement: pulmonary function testing in preschool children. *Am J Respir Crit Care Med*. 2007;175(12):1304-1345.

86. Radics BL, Gyurkovits Z, Makan G, Gingl Z, Czövek D, Hantos Z. Respiratory Oscillometry in Newborn Infants: Conventional and Intra-Breath Approaches. *Front Pediatr*. 2022;10:867883. doi:10.3389/fped.2022.867883

87. Watts JC, Farah CS, Seccombe LM, et al. Measurement duration impacts variability but not impedance measured by the forced oscillation technique in healthy, asthma and COPD subjects. *ERJ Open Res*. 2016;2(2). doi:10.1183/23120541.00094-2015

88. Kuypers K, Martherus T, Lamberska T, Dekker J, Hooper SB, Pas AB te. Reflexes that impact spontaneous breathing of preterm infants at birth: a narrative review. *Arch Dis Child - Fetal Neonatal Ed*. 2020;105(6):675-679. doi:10.1136/archdischild-2020-318915

89. Rosenfeld M, Allen J, Arets BH, et al. An official American Thoracic Society workshop report: optimal lung function tests for monitoring cystic fibrosis, bronchopulmonary dysplasia, and recurrent wheezing in children less than 6 years of age. *Ann Am Thorac Soc*. 2013;10(2):S1-S11.

90. Rzehak P, Wijga AH, Keil T, et al. Body mass index trajectory classes and incident asthma in childhood: Results from 8 European Birth Cohorts—a Global Allergy and Asthma European Network initiative. *J Allergy Clin Immunol*. 2013;131(6):1528-1536. doi:10.1016/j.jaci.2013.01.001

91. Berger KI, Kalish S, Shao Y, et al. Isolated small airway reactivity during bronchoprovocation as a mechanism for respiratory symptoms in WTC dust-exposed community members. *Am J Ind Med*. 2016;59(9):767-776. doi:10.1002/ajim.22639

92. Segal LN, Goldring RM, Oppenheimer BW, et al. Disparity Between Proximal and Distal Airway Reactivity During Methacholine Challenge. *COPD J Chronic Obstr Pulm Dis*. 2011;8(3):145-152. doi:10.3109/15412555.2011.560127

Appendix A. Questionnaires

Questionnaire

	Strongly Disagree Pas du tout d'accord	Somewhat Disagree Plutôt pas d'accord	Neutral Neutre	Somewhat Agree Plutôt d'accord	Strongly Agree Tout à fait d'accord
My baby appeared comfortable during the test / Mon bébé est apparu confortable pendant le test					
The duration of the entire test was acceptable / La durée du test était acceptable					
I would let my baby be tested again in the future / Je laisserais mon bébé être testé à nouveau dans le futur					

Comments and Suggestions / Commentaires et suggestions

Figure A1. Questionnaire for parents after testing.

Technician Questionnaire

	Strongly Disagree Pas du tout d'accord	Somewhat Disagree Plutôt pas d'accord	Neutral Neutre	Somewhat Agree Plutôt d'accord	Strongly Agree Tout à fait d'accord
The software and interface were easy to use / Le logiciel et l'interface étaient faciles à utiliser					
The setup was easy / Le montage était facile					
The calibration routine was easy / La procédure d'étalonnage était facile					
The device was easy to manipulate / L'appareil était facile à manipuler					
The cleaning was easy / Le nettoyage était facile					
The infant tolerated the testing / Le nourrisson a toléré le test					

It was easy to get a good seal over the nose and mouth / Il était facile d'obtenir un bon sceau sur le nez et la bouche					

Comments and Suggestions / Commentaires et suggestions

Figure A2. Questionnaire for device operator.

Appendix B. Email Templates

B1 Consent Email

Hello Ms. _____,

At the maternity ward, I got permission to contact you in a few weeks about participating in our research study on infant lung function. I wanted to follow up with you to see if you would still be interested in participating.

A detailed description of the study is attached to this email.

Please reply to this email to let me know if you would like to participate or not, or if you have any questions or concerns.

B2 Follow-up Email

Hello Ms. _____,

Following up on the email below, I was wondering if you got a chance to look through the document and come to a decision about participating in our research study?

Please let me know.

B3 Screening Email

Hi Ms. _____,

Thank you for agreeing to participate in our study.

Before we proceed, a few screening questions:

1. Has your baby had any respiratory infections in the prior month or been diagnosed with a chronic condition that would affect breathing (e.g. cystic fibrosis, neuromuscular disease, gastroesophageal reflux disease)?
2. Is s/he on any medication other than vitamins?

If the answer is no to all of the above, then we can book the appointment. It helps to schedule it to coincide with the baby's usual naptime, if s/he has one.

The following times are available:
Day Month Date #xm-#xm
.....
Please let me know if any of those days work for you.

B4 Appointment Email

Hi Ms. _____,

Thank you for getting back to me.

We look forward to seeing you on **Day, Date Month** at **#:##xm** at the Centre for Innovative Medicine - Pediatrics B04.3310. It is located in Zone B on the 4th floor at the Montreal Children's Hospital.

Since the test is conducted on a sleeping baby, please avoid any car ride naps on the way to the hospital. Otherwise, babies are wide awake when they arrive and take a long time to fall back asleep.

If you have any questions/concerns or can no longer make it to the appointment, feel free to reply to this email.

B5 Appointment Reminder Email

This is a friendly reminder for your appointment **tomorrow** at **#:##xm** at the Centre for Innovative Medicine - Pediatrics B04.3310. It is located in Zone B on the 4th floor at the Montreal Children's Hospital.

Since the test is conducted on a sleeping baby, please avoid any car ride naps on the way to the hospital. Otherwise, babies are wide awake on arrival and take a while to fall back asleep.

If you have any questions/concerns or can no longer make it to the appointment, feel free to reply to this email.

Appendix C. Descriptive Statistics

Table C 1. Descriptive statistics of OSC measurements from each device (SE = standard error; SD = standard deviation; SV = sample variance; min = minimum; max = maximum; CI = confidence interval)

R7				**X7**			
wave-tube		*tremoFlo*		*wave-tube*		*tremoFlo*	
Mean	51.01	Mean	35.52	Mean	-20.42	Mean	-20.13
SE	3.64	SE	1.66	SE	5.61	SE	1.07
Median	49.85	Median	36.51	Median	-17.11	Median	-20.08
Mode	#N/A	Mode	#N/A	Mode	#N/A	Mode	#N/A
SD	7.28	SD	3.31	SD	11.23	SD	2.14
SV	52.98	SV	10.99	SV	126.11	SV	4.56
Range	15.41	Range	7.03	Range	25.58	Range	5.12
Min	44.47	Min	31.02	Min	-36.52	Min	-22.74
Max	59.88	Max	38.04	Max	-10.94	Max	-17.62
Sum	204.04	Sum	142.07	Sum	-81.67	Sum	-80.50
Count	4.00	Count	4.00	Count	4.00	Count	4.00
CI (95.0%)	11.58	CI (95.0%)	5.27	CI (95.0%)	17.87	CI (95.0%)	3.40
R13				**X13**			
wave-tube		*tremoFlo*		*wave-tube*		*tremoFlo*	
Mean	49.27	Mean	28.70	Mean	-13.06	Mean	-12.41
SE	8.12	SE	0.61	SE	4.50	SE	0.57
Median	42.36	Median	28.24	Median	-10.48	Median	-12.31
Mode	#N/A	Mode	#N/A	Mode	#N/A	Mode	#N/A
SD	16.24	SD	1.22	SD	9.00	SD	1.14
SV	263.60	SV	1.48	SV	81.06	SV	1.30
Range	34.13	Range	2.64	Range	20.71	Range	2.67
Min	39.12	Min	27.84	Min	-25.99	Min	-13.84
Max	73.25	Max	30.48	Max	-5.28	Max	-11.17
Sum	197.08	Sum	114.81	Sum	-52.23	Sum	-49.64
Count	4.00	Count	4.00	Count	4.00	Count	4.00
CI (95.0%)	25.83	CI (95.0%)	1.93	CI (95.0%)	14.33	CI (95.0%)	1.82
R19				**X19**			
wave-tube		*tremoFlo*		*wave-tube*		*tremoFlo*	
Mean	44.27	Mean	26.54	Mean	-7.62	Mean	-7.15
SE	5.85	SE	1.11	SE	5.36	SE	0.93
Median	39.93	Median	27.10	Median	-3.92	Median	-6.96

Mode	#N/A	Mode	#N/A	Mode	#N/A	Mode	#N/A
SD	11.69	SD	2.22	SD	10.73	SD	1.87
SV	136.72	SV	4.92	SV	115.05	SV	3.49
Range	25.60	Range	4.90	Range	23.15	Range	4.26
Min	35.82	Min	23.54	Min	-22.88	Min	-9.47
Max	61.42	Max	28.44	Max	0.26	Max	-5.21
Sum	177.10	Sum	106.17	Sum	-30.47	Sum	-28.60
Count	4.00	Count	4.00	Count	4.00	Count	4.00
CI (95.0%)	18.61	CI (95.0%)	3.53	CI (95.0%)	17.07	CI (95.0%)	2.97
R29				**X29**			
wave-tube		*tremoFlo*		*wave-tube*		*tremoFlo*	
Mean	42.44	Mean	25.37	Mean	-0.70	Mean	-3.20
SE	4.14	SE	1.54	SE	4.81	SE	1.36
Median	40.79	Median	26.51	Median	2.22	Median	-4.07
Mode	#N/A	Mode	#N/A	Mode	#N/A	Mode	#N/A
SD	8.29	SD	3.07	SD	9.61	SD	2.72
SV	68.67	SV	9.44	SV	92.35	SV	7.39
Range	17.87	Range	6.75	Range	20.62	Range	5.97
Min	35.17	Min	20.85	Min	-13.93	Min	-5.31
Max	53.04	Max	27.60	Max	6.70	Max	0.66
Sum	169.78	Sum	101.46	Sum	-2.78	Sum	-12.79
Count	4.00	Count	4.00	Count	4.00	Count	4.00
CI (95.0%)	13.19	CI (95.0%)	4.89	CI (95.0%)	15.29	CI (95.0%)	4.33
R37				**X37**			
wave-tube		*tremoFlo*		*wave-tube*		*tremoFlo*	
Mean	40.55	Mean	25.50	Mean	2.21	Mean	0.28
SE	3.22	SE	1.57	SE	4.98	SE	1.70
Median	39.54	Median	26.50	Median	4.58	Median	0.36
Mode	#N/A	Mode	#N/A	Mode	#N/A	Mode	#N/A
SD	6.43	SD	3.13	SD	9.97	SD	3.40
SV	41.38	SV	9.82	SV	99.35	SV	11.56
Range	14.82	Range	7.00	Range	22.90	Range	7.57
Min	34.15	Min	21.00	Min	-11.61	Min	-3.59
Max	48.97	Max	28.01	Max	11.29	Max	3.98
Sum	162.21	Sum	102.00	Sum	8.85	Sum	1.10
Count	4.00	Count	4.00	Count	4.00	Count	4.00
CI (95.0%)	10.24	CI (95.0%)	4.99	CI (95.0%)	15.86	CI (95.0%)	5.41
R7-19				**R7-29**			
wave-tube		*tremoFlo*		*wave-tube*		*tremoFlo*	

Mean	6.74	Mean	8.97	Mean	8.57	Mean	10.15
SE	3.01	SE	1.09	SE	0.79	SE	0.78
Median	8.13	Median	8.51	Median	8.46	Median	10.31
Mode	#N/A	Mode	#N/A	Mode	#N/A	Mode	#N/A
SD	6.01	SD	2.18	SD	1.57	SD	1.55
SV	36.16	SV	4.77	SV	2.48	SV	2.40
Range	13.77	Range	4.76	Range	3.67	Range	3.76
Min	-1.54	Min	7.06	Min	6.84	Min	8.12
Max	12.23	Max	11.81	Max	10.51	Max	11.88
Sum	26.95	Sum	35.89	Sum	34.26	Sum	40.61
Count	4.00	Count	4.00	Count	4.00	Count	4.00
CI (95.0%)	9.57	CI (95.0%)	3.47	CI (95.0%)	2.51	CI (95.0%)	2.47
f_{res}				**AX**			
wave-tube		*tremoFlo*		*wave-tube*		*tremoFlo*	
Mean	16.33	Mean	15.46	Mean	261.06	Mean	228.60
SE	6.01	SE	9.02	SE	141.98	SE	21.55
Median	18.18	Median	13.82	Median	142.48	Median	232.48
Mode	#N/A	Mode	0.00	Mode	#N/A	Mode	#N/A
SD	12.02	SD	18.05	SD	283.95	SD	43.09
SV	144.56	SV	325.65	SV	80629.57	SV	1856.81
Range	28.97	Range	34.18	Range	599.89	Range	101.18
Min	0.00	Min	0.00	Min	79.69	Min	174.13
Max	28.97	Max	34.18	Max	679.58	Max	275.32
Sum	65.33	Sum	61.82	Sum	1044.24	Sum	914.41
Count	4.00	Count	4.00	Count	4.00	Count	4.00
CI (95.0%)	19.13	CI (95.0%)	28.71	CI (95.0%)	451.83	CI (95.0%)	68.57
R16				**X16**			
wave-tube		*tremoFlo*		*wave-tube*		*tremoFlo*	
Mean	42.03	Mean	25.97	Mean	-11.17	Mean	-9.65
SE	4.70	SE	0.89	SE	3.33	SE	0.81
Median	46.46	Median	26.69	Median	-9.21	Median	-9.63
Mode	#N/A	Mode	#N/A	Mode	#N/A	Mode	#N/A
SD	8.13	SD	1.54	SD	5.77	SD	1.41
SV	66.14	SV	2.38	SV	33.28	SV	1.98
Range	14.35	Range	2.82	Range	11.03	Range	2.82
Min	32.65	Min	24.19	Min	-17.67	Min	-11.07
Max	46.99	Max	27.01	Max	-6.64	Max	-8.25
Sum	126.09	Sum	77.90	Sum	-33.52	Sum	-28.96
Count	3.00	Count	3.00	Count	3.00	Count	3.00
CI (95.0%)	20.20	CI (95.0%)	3.83	CI (95.0%)	14.33	CI (95.0%)	3.50